

Non-Synthetic Polymer Biomodification using Gold Nanoparticles

Bachelors of Science Honors Thesis

Presented in Partial Fulfillment of the Requirements for Graduation with Distinction in Chemical
and Biomolecular Engineering from The Ohio State University

By

Craig Buckley

The Ohio State University

May 2009

Honors Thesis Committee:

Dr. Jessica Winter, Advisor

Dr. David Tomasko

Acknowledgments:

I would like to thank Michael Boehm for his expertise and assistance in the rheological aspects of the project. I would also like to thank Katie Vermeersch for her contributions to the biosensing and cell studies portions of this work and Dr. Winter and the members of the Winter Lab for their helpful advice over the last two years.

Abstract

Tissue engineering, the creation of replacement tissue using natural and synthetic components, requires the ability to manipulate the local chemical environment of polymeric biomaterials, which are materials designed to augment or replace natural functions. Many polymeric biomaterials display excellent mechanical characteristics and compatibility to native tissue, but they do not readily support cell adhesion. Unfortunately, modification of these materials can be difficult. For example, agarose and poly (ethylene glycol) diacrylate (PEGDA) hydrogels only weakly support cell growth, and cell adhesion molecules must be added to improve the cell-material interface. Methods to chemically modify agarose and PEGDA hydrogels have been developed, but these methods tend to be difficult and time consuming. A new technique for modification, using gold nanoparticles embedded within a hydrogel matrix, offers a solution to these problems. The particles serve as attachment points for cell adhesion peptides to facilitate bioconjugation. These methods can be applied to many types of hydrogels with different pore sizes simply by changing the nanoparticle size, as opposed to developing novel synthetic chemistry. Several sizes of gold nanoparticles have been synthesized, entrained in agarose hydrogels, and tested to show that the bulk of particles remain in the gel for a substantial length of time. Mechanical properties of the gold nanoparticle composite hydrogels are similar to the unmodified hydrogels, retaining the native material characteristics. A cell-binding peptide has successfully been conjugated to gold nanoparticles, and the effect of this binding peptide on cell growth and adhesion is being studied by culturing cells on the unmodified and composite hydrogels. Although the initial results are promising, more testing is necessary to quantify the extent of adhesion in each case. The composite gels being examined offer many advantages over the previous methods of polymeric bioconjugation. The chemistry is simple and robust, the gel's polymeric backbone and mechanical properties are preserved, and the modification technique can be applied to a wide range of biomaterials. Because of this flexibility, this technology is not limited to a single component or tissue type, but can be applied to all areas of tissue engineering, providing novel methods of non-synthetic bioconjugation.

In addition to biomodification, these materials offer the opportunity for integrated sensing, due to the well recognized optical properties of gold nanoparticles. Biosensor detection is based on the absorbance shift resulting from surface plasmon resonance (SPR) experienced by aggregated

gold nanoparticles. For example, two bound gold nanoparticles experience a SPR-induced absorbance shift as a result of proximity. When the particles are separated, the absorbance returns to its original value. In a proof-of-concept device, particle aggregation is achieved using a modified cell binding peptide (CGGGRGDSGGGC), whereas cleavage is produced by an enzyme that promotes cell detachment (trypsin), returning particles to their initial unaggregated state. Particles are also modified with tri(ethylene glycol) mono-11-mercaptoundecyl ether, a stabilizing agent that protects the particles from unwanted aggregation. Although this proof-of-concept system examines cell adhesion using the RGD peptide/trypsin protease system, the biosensor could be customized to almost any enzyme-substrate combination. Any substrate with thiol ends (which can be added through cysteine termination) has the ability to bind the gold nanoparticles together, and any substrate specific enzyme can cleave the peptide bond activating the sensor. Thus, analyte sensing can be directly built into a modified hydrogel by integrating the prepared gold nanoparticles during gel synthesis.

The general modification method described here has numerous advantages. Both the increased biocompatibility and sensing applications of gold nanoparticle-biomaterial composites are improvements over systems based solely on hydrogels and polymers or just nanoparticles alone. The combined system provides the hydrogel biomaterials with increased functionality without the requirement of complicated syntheses. In addition, the nanoparticles are provided with a supportive framework. Some of the most promising biosensor models employ aqueous nanoparticles, which are not inherently portable and operate only in the liquid phase. A hydrogel support permits the development of portable devices with potential for gas phase operation. The methods described here are also very flexible as a result of the ability to functionalize the gold nanoparticles with a wide array of biomolecules, providing a composite system with a variety of features.

Table of Contents

1. Introduction.....	1
2. Background.....	5
2.1 Polymer Biomodification.....	5
2.2 Biosensors.....	15
3. Cell Adhesion.....	19
3.1 Introduction.....	19
3.2 Experimental.....	22
3.2.1 Gold Nanoparticle Synthesis.....	22
3.2.2 Gold Nanoparticle Characterization.....	23
3.2.3 Gold Nanoparticle – Hydrogel Composite Creation.....	23
3.2.4 Elution Tests.....	24
3.2.5 Rheological Tests.....	25
3.2.6 Cell Studies.....	26
3.2.6.1 Preparing Sterile Agarose Gels.....	26
3.2.6.2 Preparing Sterile Composite Gels for Cell Adhesion Tests.....	27
3.2.6.3 Culturing Cells on the Composite Gels.....	29
3.2.6.4 Cell Adhesion Experiment Modifications.....	29
3.2.6.5 PEGDA Cell Adhesion Experiments.....	30
3.3 Results and Discussion.....	32
3.3.1 Gold Nanoparticle Characterization.....	32
3.3.2 Gold Nanoparticle – Hydrogel Composites.....	35
3.3.3 Elution Test Results.....	36
3.3.4 Rheological Test Results.....	38
3.3.5 Cell Studies Results.....	40
3.4 Conclusions.....	50
4. Biosensor.....	52
4.1 Introduction.....	52
4.2 Experimental.....	54
4.2.1 Initial Peptide Tests.....	54
4.2.2 Stabilizing Ligand Tests.....	54
4.2.3 Optimizing Stabilizing Ligand Concentration.....	55
4.3 Results and Discussion.....	56
4.3.1 Initial Peptide Tests.....	56
4.3.2 Stabilizing Ligand Tests.....	58
4.2.3 Optimizing Stabilizing Ligand Concentration.....	60
4.4 Conclusions.....	65
5. Overall Conclusions.....	66
6. Recommendations for Future Work.....	68
7. References.....	69

List of Figures

Figure 1.1: Deep Brain Stimulation Electrode.....	1
Figure 2.1: Cell Behavior Depends on Substrate Stiffness.....	6
Figure 2.2: Agarose Structure, Gelation Process, Image, and SEM.....	7
Figure 2.3: CDI based CDPGYIGSR modification of Agarose	8
Figure 2.4: Chick DRG Cells Grown in Unmodified and Modified Agarose	9
Figure 2.5: PC 12 Cells Extending Neurites in Several Types of Modified Agarose	9
Figure 2.6: Formation of PEGDA Hydrogels.....	10
Figure 2.7: HASMC's in AAAAAAAAAAK-conjugated and Unmodified PEGDA Hydrogels...	11
Figure 2.8: AFM Image of RGD Modified Alginate Hydrogel with Conjugated 5 nm Gold Nanoparticles	12
Figure 2.9: Relative Uptake of Transferrin-Coated Gold Nanoparticles.....	13
Figure 2.10: Dependence of Absorbance on Gold Nanoparticle Size (diameter – in nm)	15
Figure 2.11: Reversible Aggregation of Gold Nanoparticles with a Dithiol Linker	16
Figure 2.12: Gold Nanoparticles in Presence of Treated and Untreated Peptide (original)	17
Figure 2.13: Gold Nanoparticle – Quantum Dot Based Biosensor.....	18
Figure 3.1: Schematic of a Single Functionalized Gold Nanoparticle (left) with the Structure of the Adhesion-Promoting Peptide CDPGYIGSR (right).....	20
Figure 3.2: Diagram of a Gold Nanoparticle Composite Hydrogel Interacting with a Nearby Cell (not to scale).....	21
Figure 3.3: Gold Nanoparticle Elution Experiment Sketch (left – profile view of well plate; right – top view of well plate with one gel concentration set of samples shown).....	25
Figure 3.4: Rheometer Setup with Hydrogel Sample	26
Figure 3.5: Gels Created for Cell Adhesion Pilot Experiments.....	28
Figure 3.6: Experimental Setup for Initial Cell Adhesion Experiments.....	30
Figure 3.7: Absorbance Spectrums of DMAA synthesized and Commercial 90 nm Gold Nanoparticles	32
Figure 3.8: DMAA Gold Nanoparticles Dynamic Light Scattering Results	33
Figure 3.9: “Nanopartz” 90 nm Gold Nanoparticles Dynamic Light Scattering Results	34
Figure 3.10: SEM Comparison of DMAA and “Nanopartz” 90 nm Gold Nanoparticles	34
Figure 3.11: Comparison of Modified and Unmodified Agarose Hydrogels	35
Figure 3.12: Seaprep Agarose Hydrogels with Increasing Gold Nanoparticle Concentration.....	35
Figure 3.13: Nanopartz 90 nm Particle Elution in Seaprep (SP) Agarose – Gel Absorbance Measurements	37
Figure 3.14: Composite Seaprep Agarose (1x) Hydrogel after 13 Days in PBS.....	37
Figure 3.15: Storage Modulus for Composite 1.5% Seaprep Agarose Hydrogels	39
Figure 3.16: Loss Modulus for Composite 1.5% Seaprep Agarose Hydrogels.....	40
Figure 3.17: Phase Contrast and LIVE/DEAD Staining Images of PC12 cells in a Test Well....	41
Figure 3.18: 6 Well Plate Experiment Images – 1.5% Agarose (1x Au NP's).....	45
Figure 3.19: Experimental Gel from Transwell Inserts	46
Figure 3.20: PC12 Cells Grown on Transwell Insert Surface	46
Figure 3.21: PEGDA Hydrogel (1x Au NP's) Cell Adhesion Images	48
Figure 3.22: Experimental Composite PEGDA hydrogel (Au NP's and peptide)	49

Figure 4.1: Peptide Binding Mechanism of Gold Nanoparticle Biosensor	53
Figure 4.2: Converting Biosensor to Gel Basis and Sensing in Solution	53
Figure 4.3: Absorbance Curves for Biosensor Peptide Addition.....	57
Figure 4.4: Comparison of Unmodified and Modified Gold Nanoparticles.....	57
Figure 4.5: Unmodified and 15 nm Gold Nanoparticle Modified PEGDA Hydrogels	58
Figure 4.6: Schematic of Stabilizing Ligand Properties (ligand in gray, peptide in black).....	58
Figure 4.7: Structures of Unsuccessful Ligands	59
Figure 4.8: Tri(ethylene glycol) mono-11-mercaptoundecyl ether (ME).....	60
Figure 4.9: Combined Effect of ME and PBS on 15 nm Gold Nanoparticles.....	61
Figure 4.10: Absorbance Spectrums with No ME and Increasing PBS	63
Figure 4.11: Absorbance Spectrums with 8×10^{-8} M ME and Increasing PBS.....	63
Figure 4.12: Absorbance Spectrums with 8×10^{-6} M ME and Increasing PBS.....	64
Figure 4.13: Normalized Absorbance Spectrums with ME and Peptide added.....	64

1. Introduction

The study of how cells grow and develop is essential for fields such as tissue engineering where the eventual goal is to restore lost function and regenerate damaged tissues and organs. One way in which this is done is through the creation of novel biomaterials. In some cases, the biomaterial may be used directly as a replacement tissue, such as with artificial skin and heart valves. In other cases, the biomaterial may be used to coat biomedical implants so as to improve their biocompatibility. One specific example of this use is seen in neurodegenerative research. Although drug treatment remains popular for Parkinson's disease, the second most common neurodegenerative disorder and effecting 2% of those over the age of 60, its effectiveness is limited as the disease progresses.¹ To compensate for this, deep brain stimulation through probes implanted directly into the brain is becoming more common as a treatment for advanced Parkinson's disease.² One such probe is shown in Figure 1.1. However, the usefulness of this treatment also diminishes over time as the immune response to the probe can cause neuronal death in the surrounding tissue, resulting in increased electrical resistance and a decrease in performance. This is a common problem among neural implants, and developing a way to better interface the foreign probe with the body's natural cells is vital for their continued effectiveness.

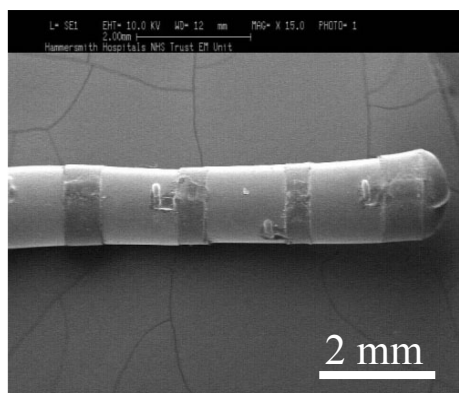


Figure 1.1: Deep Brain Stimulation Electrode³

A necessary requirement for improving biomedical devices like these probes and to study tissue engineering is the development of an ideal testing environment. This goal can be achieved through the three dimensional study of cells, as this allows for simulating an environment that is much closer to *in vivo* than a traditional culture dish. As different tissue types (brain, muscle, skin, etc.) have different strength and stiffness, a cell will only behave naturally in an environment with similar mechanical properties as its native one. Therefore the best environment to study a cell in is one that matches its natural state as closely as possible. At present, this is done through the use of hydrogels and polymers of varying consistencies so as to best mimic the *in vivo* stiffness that a cell “feels.”

Many potential biomaterials, while mechanically suitable for cell growth, do not readily support the adhesion of those cells. Further modification is necessary in order to make the materials into an ideal growth platform. Although this has been achieved by chemically integrating adhesion promoting and other bio-active peptides into the polymer matrix of the material, this method does have several limitations. The procedures often involve a series of chemical synthesis steps, leading to a low final yield of the bioactive molecule to be attached. The chemistry is also unique to each biomaterial, meaning that modifying two different materials with the same molecule can require vastly different approaches with varying outcomes. A potential solution to these problems is the use of gold nanoparticle – biomaterial composites. The gold nanoparticles serve as anchors within the polymer structure for the same biomolecules that would normally be chemically bound to the polymer structure. Instead the biomolecules are attached to the gold nanoparticles through a simple thiol-Au bond, and the particles are physically mixed into the polymer structure, providing the polymer with the advantages of the biomolecules without the complications of chemically integrating the molecules into the polymer

matrix. This approach can also be used to modify several types of biomaterials without any significant changes in the chemistry used or to modify materials that may not be able to be chemically altered without losing their fundamental properties. Although the size of the nanoparticles will need to be tuned to match the pore size of the polymer to be modified, this is a small price to pay for the ability to modify almost any polymer. The use of the gold nanoparticles also offers the additional advantage of being able to control biomolecule loading on the particles as well as the particle concentration itself in order to further tune the material for maximum cell compatibility.

The proposed approach for modifying biomaterials has a variety of applications beyond creating a suitable 3-D cell culture platform. These same biomaterials could potentially be used to coat the previously mentioned biomedical implants to provide a more compatible interface with the body's native tissue. The use of the gold nanoparticles within the biomaterials also allows for the possibility of integrated biosensing in a polymeric material. Most biosensors are in the unsupported liquid phase, limiting their potential applications. Integrating biosensing technology into a hydrogel or polymer can create a portable, easy to use sensor. Gold nanoparticles are well suited for the task of forming these integrated sensors due to their unique optical properties. These optical characteristics are controlled by their surface plasmon resonance (SPR) of the particles, and two small nanoparticles in close enough proximity to one another will take on the absorbance properties of a large particle while retaining their other key characteristics. By combining two small gold nanoparticles with a peptide linking molecule, a biosensor can be created. The sensor is triggered through the addition of a protease that will cleave the linking peptide, releasing the bound gold nanoparticles and returning the solution to its original color. The middle sequence of the linking peptide is chosen to react to a specific

protease, creating a biosensor tuned to the presence of that protease. Based on the previously described technique, composite biomaterials can again be created by combining the sensing-modified gold nanoparticles with a suitable polymer. In this way, the polymer gains the biosensing properties of the gold nanoparticles. A small polymer disc sensor could be created, for example, that would react to a certain protease when dropped in a solution. If the disc changed color, then the protease was present at a certain level. Future refinement could also produce composite sensors with the ability to detect airborne proteases, such as the lethal factor protein found in anthrax.

Creating composite gold nanoparticle modified biomaterials offers a potentially powerful and flexible solution to the problem of integrating additional properties into these materials in a simple manner without the negative side effects of chemically changing polymer structures. Using the gold nanoparticles as anchors for cell adhesion peptides allows for the creation of an ideal 3-D cell culturing environment for studying cells in an *in vivo* fashion as well as for coating biomedical implants to improve biocompatibility with native tissue. The composite materials may also serve as scaffolds for tissue engineering applications. The ability to integrate biosensing into the materials represents another potentially powerful application of this nanoparticle modification technique.

2. Background

2.1 Polymer Biomodification

In order to create a gold nanoparticle composite biomaterial for biological applications, the appropriate base material must first be chosen. This is important because of the way that the cells interact with their surroundings. It has been shown with fibroblast cells, for example, that their morphology and migration differ once suspended in 3-D collagen gels versus 2-D cultures.⁴ Normal tissue cells are not viable when suspended in fluid and need adhesion to some solid. While attached, cells push and pull on their surroundings and respond to force from those surroundings, allowing them to “sense” substrate stiffness.⁵ The resulting behavior of the cell based on the sensed stiffness can vary widely, as demonstrated by Discher in Figure 2.1. The same type of cell exhibits very different adhesions and cytoskeletal structure based simply on being cultured in a soft versus a stiff matrix. In the lower portion of the figure, muscle cells are only appropriately differentiated and show the proper striation when cultured on top of an existing cell layer. This lower layer was cultured first on a glass slide and is also the same type of cell but did not differentiate in the usual manner because of the influence of the stiff glass surface. This behavior serves to illustrate the importance of choosing the appropriate biomaterial for any cell study or biomedical application as well as reinforcing the need to avoid affecting the mechanical properties of the chosen material when biomodifications are made.

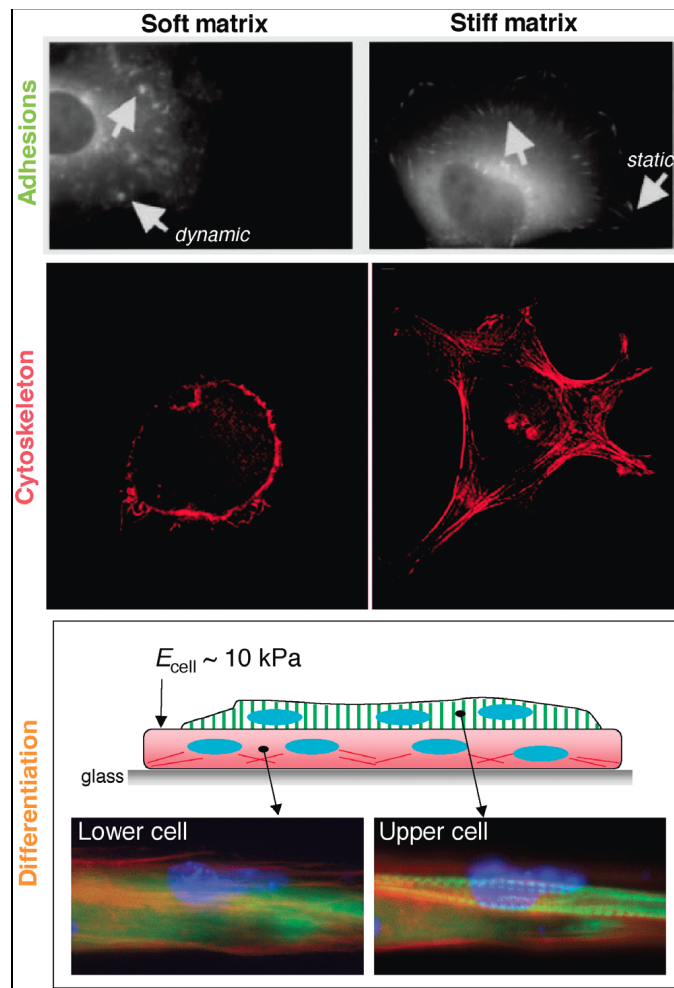


Figure 2.1: Cell Behavior Depends on Substrate Stiffness ⁵

Due to its softness and transparency, agarose is a common brain tissue mimetic used for studying the behavior of neural-type cells. It is a physical entanglement hydrogel made up of polysaccharides which can be dissolved from a solid powder into an aqueous solution heated to 65-70° C, although higher temperatures help with dissolving high concentrations. Once the agarose is fully dissolved, the solution will gel once appropriately cooled, with lower temperatures being required for lower gel concentrations. The resulting gel can then be heated to about 40° C before it begins to melt. Figure 2.2 demonstrates this process, where the solid agarose chains are able to coil and entangle once dissolved in solution, eventually solidifying into a solid gel. The gel, however, is still over 90% water and has a very fibrous pore structure,

as shown by the scanning electron micrograph. The mean pore diameter of a 1.5 wt % agarose hydrogel is approximately 66-88 nm, which is on the larger end for a polymer but not excessively large that nanoparticles can't remain entrapped within the structure.⁶ Pore size continues to decrease with increasing agarose concentration.

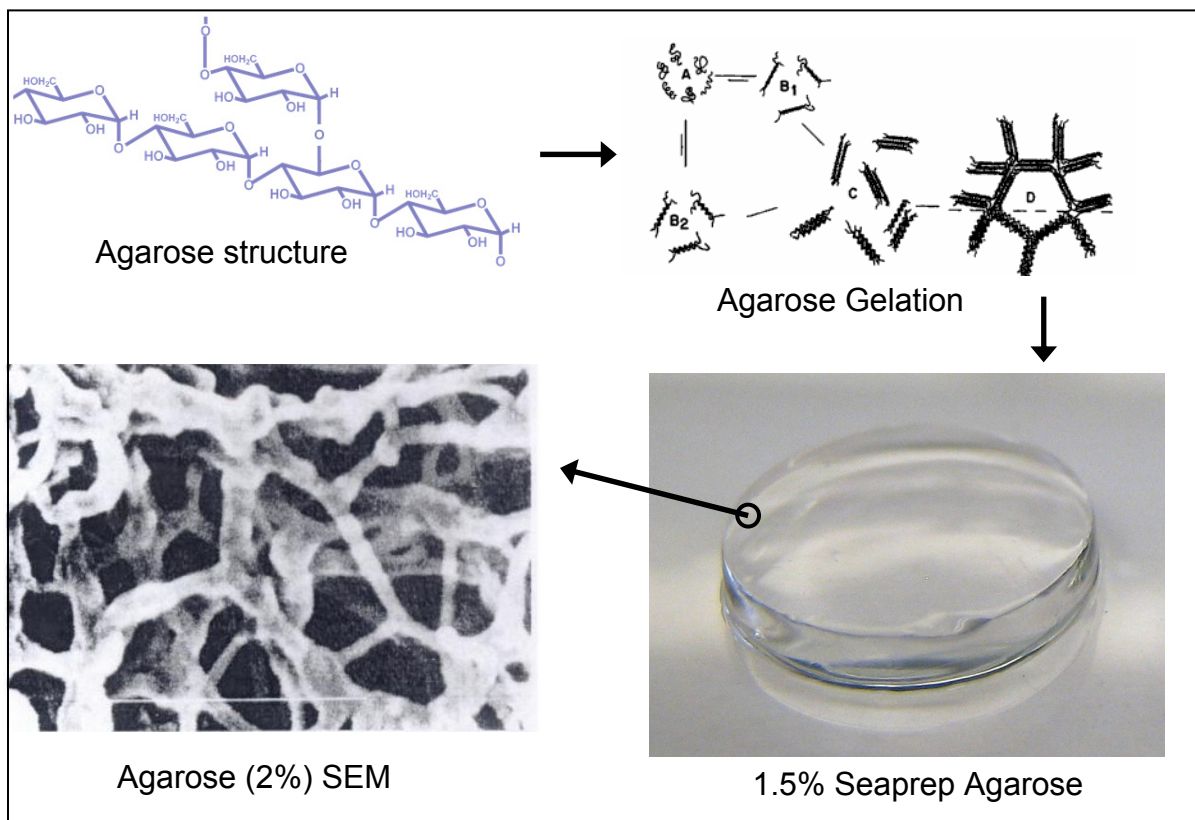


Figure 2.2: Agarose Structure, Gelation Process⁷, Image, and SEM⁷

Agarose has previously been chemically modified by Ravi Bellamkonda's group with the CDPGYIGSR fragment of the cell adhesion peptide Laminin using an imidazole coupling agent to link the peptide to the hydroxyl backbone of agarose.⁸ The coupling chemistry is shown in Figure 2.3, where a carbonyldiimidazole (CDI) group first reacts with a hydroxyl group on the agarose backbone, activating that site. The amine group on the cysteine end of the peptide reacts with the free end of the CDI, completing the conjugation. Figure 2.3 describes this process.

Agarose and peptide coupling chemistry

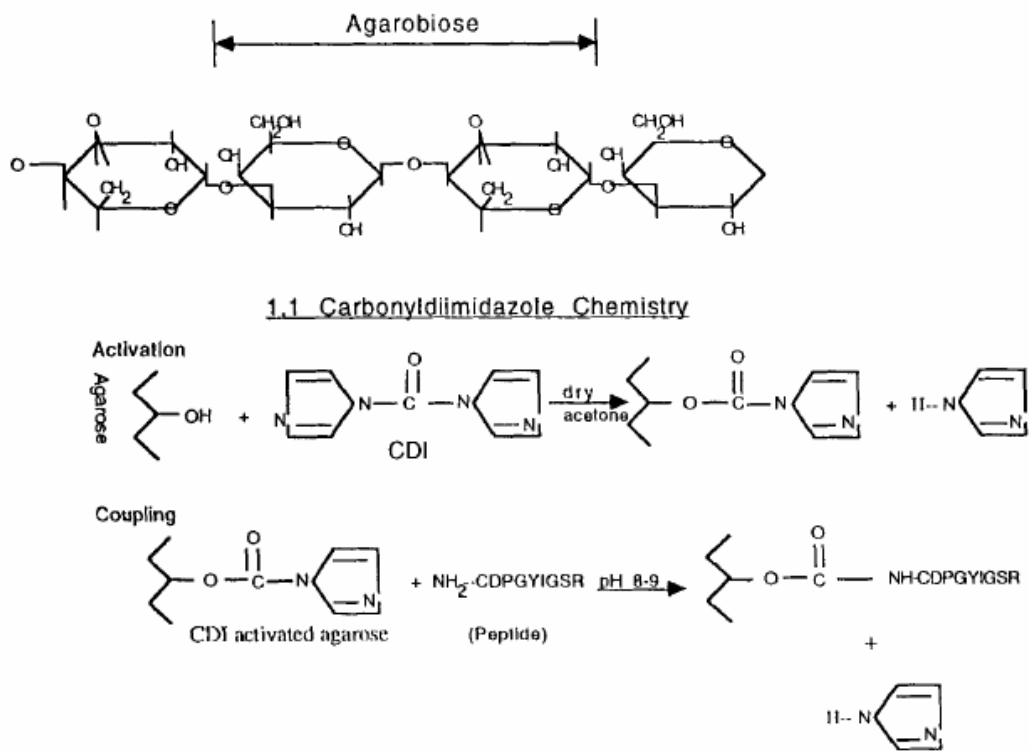
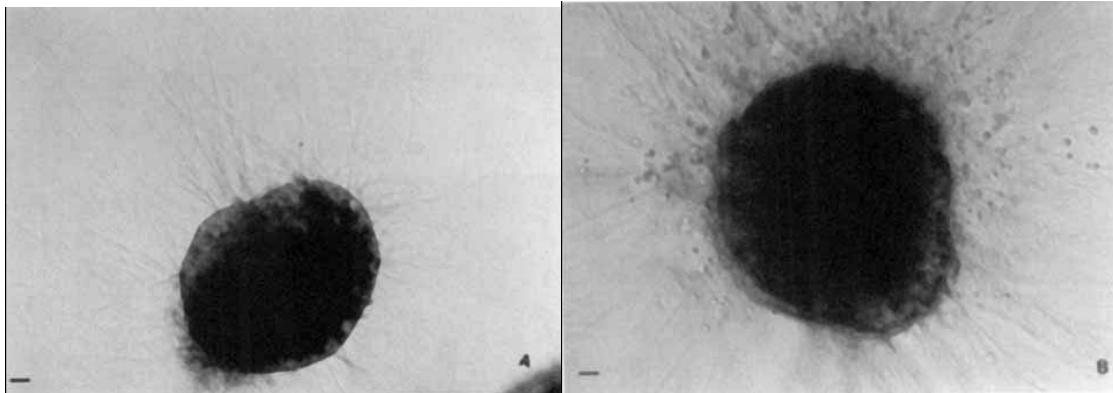


Figure 2.3: CDI based CDPGYIGSR modification of Agarose ⁸

After the agarose was modified with the CDPGYIGSR peptide, chick dorsal root ganglion (DRG) cells were encapsulated in both modified and unmodified agarose and their neurite extension compared. Figure 2.4 shows that the neurite extension was clearly improved in the modified agarose. PC12 cells (neuroprogenitor cells that express a neural phenotype in the presence of nerve growth factor) were also cultured in CDPGYIGSR modified and unmodified agarose and counted to determine the number extending neurites. This is shown in Figure 2.5. Additional peptide modifications of agarose were also compared for reference. All modifications performed significantly better than unmodified agarose, but most samples still had below 10% of their cells extending neurites.



After 6 days in unmodified agarose

After 6 days in CDPGYIGSR modified agarose

Figure 2.4: Chick DRG Cells Grown in Unmodified and Modified Agarose⁸

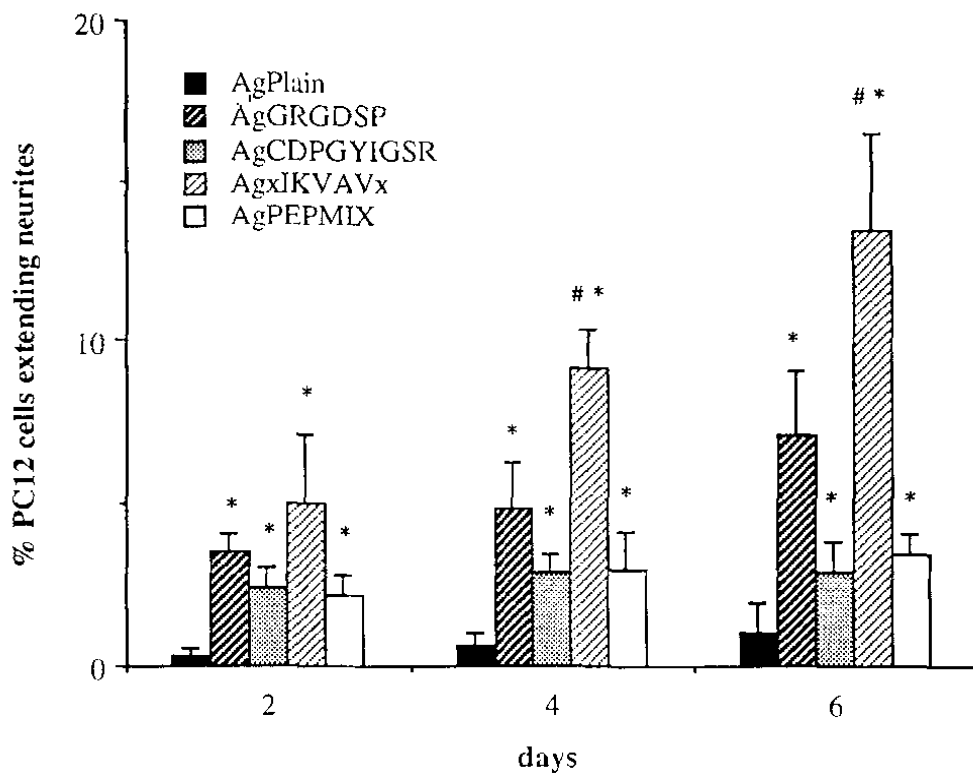


Figure 2.5: PC 12 Cells Extending Neurites in Several Types of Modified Agarose⁸

Poly(ethylene glycol) diacrylate (PEGDA) is another example of a potential biomaterial that has been chemically modified to make it more biocompatible. In contrast to agarose, PEGDA is a UV photopolymerization polymer created by the free-radical initiated polymerization of individual PEGDA molecules, as shown in Figure 2.6. PEGDA is a much stiffer hydrogel than

agarose in general and is more suited to muscle rather than neuronal cells, although its properties can vary with the chain length of PEGDA used.

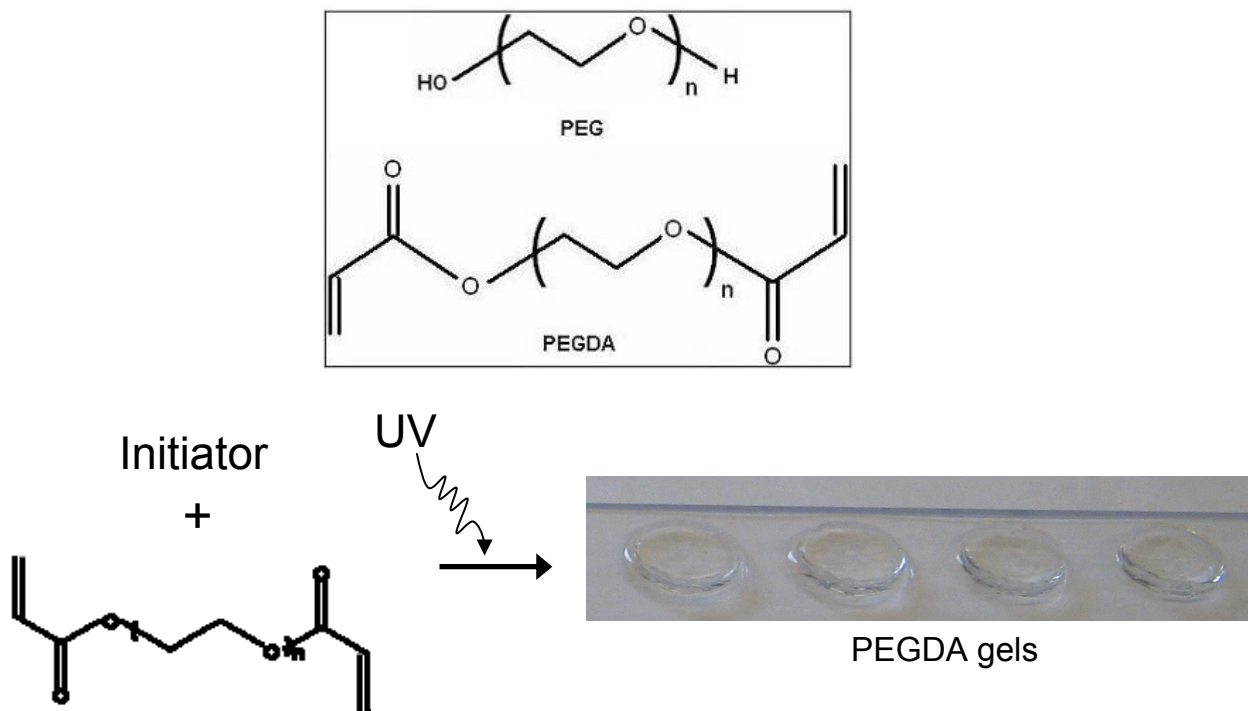
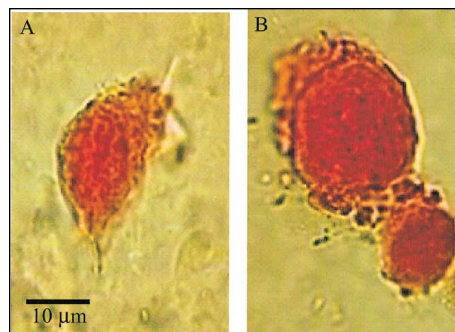


Figure 2.6: Formation of PEGDA Hydrogels

An example of a modification previously performed on PEGDA hydrogels is the incorporation of the degradable peptide sequence AAAAAAAAAAK by Jennifer West's group.⁹ By reacting this peptide with acryloyl-PEG-*N*-hydroxysuccinimide, a PEG-monoacrylate chain was added to both ends of the peptide which allowed the peptide to be incorporated into the PEGDA polymer chain during photopolymerization. Human aortic smooth muscle cells grown in AAAAAAAAAAK derivatized hydrogels were able to extend processes and begin migratory behavior since they could cleave the polyalanine sequence (see Figure 2.7). In contrast, the cells in unmodified PEGDA hydrogels were unable to achieve the same behavior due to their inability to degrade the PEGDA.

AAAAAAAAAAK-
derivatized PEGDA
hydrogels



PEGDA hydrogels

Figure 2.7: HASMC's in AAAAAAAAAAK-conjugated and Unmodified PEGDA Hydrogels⁹

Two examples have been shown where a hydrogel has been chemically modified in such a way that cells cultured in those hydrogels have exhibited more *in vivo*-like behavior than in the unmodified gels. Although the techniques were successful, they were unique to each type of hydrogel to be modified and required lengthy reaction times maintained under specific conditions not fully described here. In contrast, the proposed gold nanoparticle modification technique offers the potential to modify any type of hydrogel or polymer in the same fashion with additional control. By attaching the same adhesion-promoting peptides to the gold nanoparticles, the particles themselves serve as anchors within the hydrogel pore structure for the peptides that neighboring cells will link to. Gold nanoparticles have been shown to be distinctly visible and separate from a hydrogel structure even when physically tethered to the structure.¹⁰ Figure 2.8 shows an AFM image collected by David Mooney's group of 5 nm gold nanoparticles conjugated to an alginate hydrogel. While these nanoparticles were much smaller than the pore structure of the gel, their ability to remain distinct and detectable supports the idea of using even larger gold nanoparticles entrained within hydrogel pores.

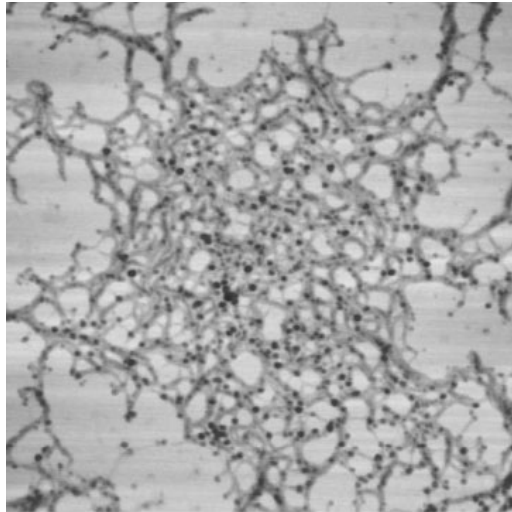


Figure 2.8: AFM Image of RGD Modified Alginate Hydrogel with Conjugated 5 nm Gold Nanoparticles¹⁰

A potential problem with the gold nanoparticle modification approach is the possibility for the gold nanoparticles to be endocytosed by the neighboring cells, as this behavior has been observed with free particles in solution. Transferrin-coated gold nanoparticles were taken up by three different types of cells (STO, HELA, SNB19) in a size specific fashion, as described by Chan in Figure 2.9.¹¹ While nanoparticles of all sizes were endocytosed, the 50 nm size range was favored over the high and low ends of the 14-100 nm range. As also shown in the figure, the particle endocytosis can be captured via TEM. Although free nanoparticles were taken up by the various cell types, they were also transferrin coated, allowing a receptor mediated endocytosis to take place. In the proposed cell adhesion application, the cell adhesion binding ligand could also potentially promote this same sort of endocytosis. However, if the particle size is sufficiently large for a given hydrogel, the cell could have difficulty pulling the particles out of a tight network unless a polymer is chosen that the cell can specifically digest. While size-tuning can be used to minimize the potential for endocytosis by avoiding particle sizes near 50 nm, the possibility still exists that a large number of particles could be collected by the cells. Another

method to help avoid such behavior would be to coat the particles with additional ligands that introduce non-specific interactions (through charge or the hydrophobic/hydrophilic nature of the ligands) to help prevent particle uptake by the cells. The sheer number of particles available in a given modified hydrogel should also be sufficiently large that even if a number are lost to endocytosis, enough will remain around any given cell to promote adhesion.

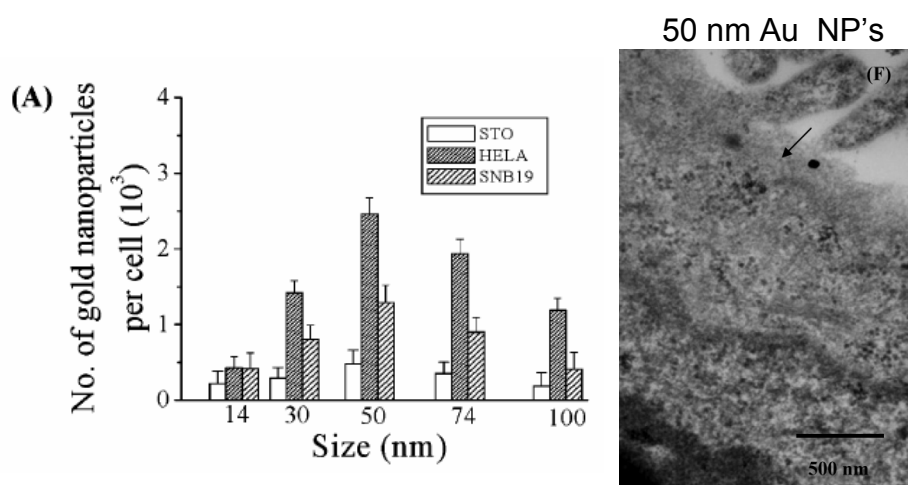


Figure 2.9: Relative Uptake of Transferrin-Coated Gold Nanoparticles¹¹

Because of the importance of size on the gold nanoparticles, the necessary techniques to synthesize those particles should also be considered. Although gold nanoparticles are commercially available from a variety of suppliers, such as Ted Pella and Nanopartz Inc., the chemical history and exact ligand composition of these samples is usually proprietary. If complete control is desired, gold nanoparticles must be synthesized in the laboratory. While a reduction of gold salts using sodium citrate is commonly used, it is best suited for making small (10-40 nm) gold nanoparticles. However, a technique using *N,N*-dimethylacetoacetamide (DMAA) is available that can synthesize roughly spherical gold nanoparticles at 20°C with decreasing particle size as reaction temperature is increased.¹² At an upper range of 100°C, approximately 20 nm particles are made but with an increase in particle geometries to include

triangular, square, and hexagonal shapes as well as spherical ones. A combination of this technique with the more standard citrate reduction techniques for the smaller sized particles (if greater monodispersity is desired) will allow for the production of gold nanoparticles over the most common potential size ranges for creating the desired nanoparticle-polymer composites.

2.2 Biosensors

Gold nanoparticle biosensors offer key advantages through increased biocompatibility and a method of simple visual recognition of sensing, although this takes place at the cost of some of the resolution found in other types of biosensors. The gold nanoparticle biosensors work based off of the absorbance shifts that gold nanoparticles can experience, which is a function of their surface plasmon resonance. Due to their unique size, gold nanoparticles selectively absorb and reflect certain wavelengths in the visible range of light. This range depends on the size of the particles, with roughly spherical gold nanoparticles less than ~40 nm in diameter appearing red and shifting in color from pink to purple as the size of the particles increases. This is demonstrated in Figure 2.10. The same color-shifting effect can be achieved by bringing two smaller gold nanoparticles together so that their absorbance properties behave as if the smaller particles were a larger single particle. This effect lasts only as long as the particles are in sufficient proximity to each other, enabling the creation of a sensing mechanism.



→ Increasing Particle Size →

Figure 2.10: Dependence of Absorbance on Gold Nanoparticle Size (diameter – in nm)¹³

This sensing mechanism has previously been demonstrated by Scrimin *et al* by first stabilizing 12 nm gold nanoparticles with a monothiol and then binding them together with a dithiol cleavable by hydrazine.¹⁴ The bound particles shift in absorbance from near 520 nm (appearing

red) to a new peak near 600 nm (appearing purple). Presence of hydrazine cleaves the dithiol, allowing the bound particles to split and return to their original state, reverting to a red color. The schematic of this process is included as Figure 2.11. This sensing mechanism is an “on sensor,” since the particles are changed to a new state (“off”) and return to their original state (“on”) in the presence of a specific substance.

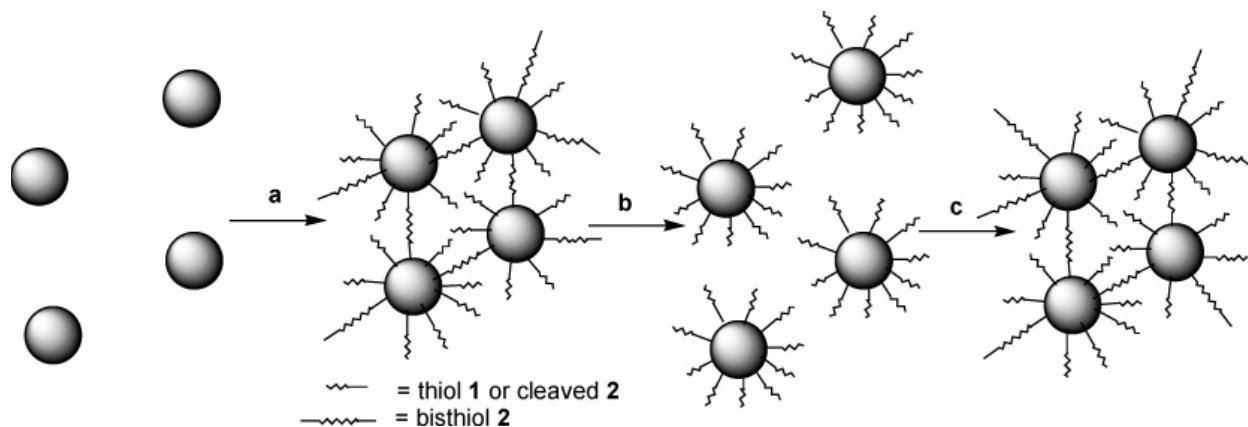


Figure 2.11: Reversible Aggregation of Gold Nanoparticles with a Dithiol Linker¹⁴

Gold nanoparticle “off” sensors have also been demonstrated by Scrimin *et al*, where the change in the sensor first occurs with detection and takes the particles away from their default state rather than returning to it.¹⁵ In this technique, a peptide with cysteine groups on either end (to provide the necessary thiol linking groups) is first reacted with the test solution before addition to the gold nanoparticles. If the test solution contains a protease capable of cleaving the peptide, the gold nanoparticle solution will be unchanged by the addition of the peptide solution since the linking groups will have been cleaved into monothiol fragments. If the protease is not present, the particles will undergo an absorbance shift as the linking peptide binds them together. This method has been demonstrated by detecting thrombin (present in blood coagulation) and lethal factor (a component of the anthrax toxin) in the low nanomolar range. Figure 2.12 illustrates the technique and shows the distinct solution color change for a positive detection.

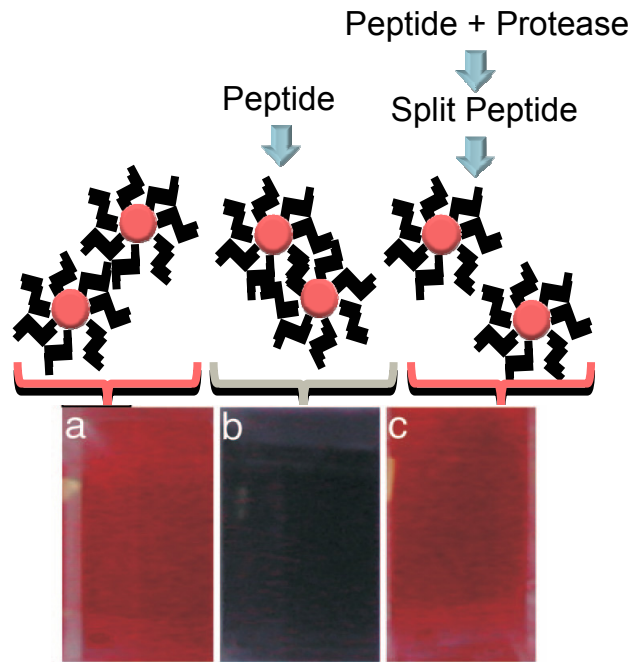


Figure 2.12: Gold Nanoparticles in Presence of Treated and Untreated Peptide (original¹⁵)

Current gold nanoparticle solution based methods of biosensing are not limited strictly to this one type of nanoparticle but can incorporate other particles as well. Peptide linked gold nanoparticle – quantum dot biosensors have been created by West *et al* that rely on the ability of the gold nanoparticles to quench the photoluminescence of the quantum dots when in their close proximity bound state.¹⁶ The CGLGPAGGCG collagenase-degradable peptide sequence was used to tie the two particle types together. In this state the quantum dots will not exhibit photoluminescence, but once the collagenase is added, the peptide is cleaved, separating the two particles and allowing the quantum dots to luminesce. This process is shown in Figure 2.13. This method of sensing is also considered an “on sensor” since the default state of the particles is “off” (no luminescence), and it is converted to “on” (luminescence) once sensing takes place. This sensor has the advantage of the ease of detecting quantum dots, which translates to a high

resolution, but quantum dots are not generally biocompatible and require a fluorescent source before they luminesce.

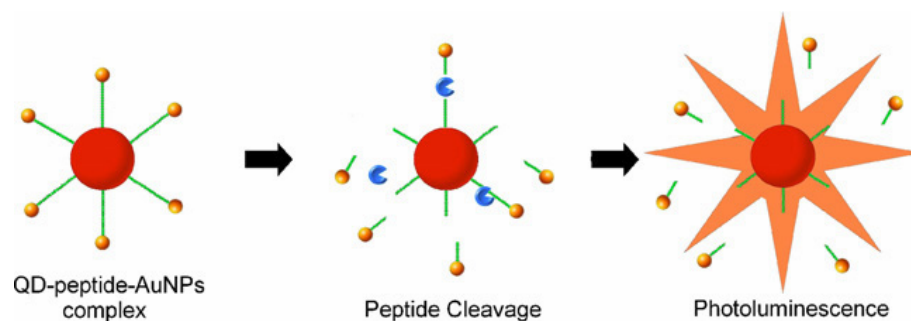


Figure 2.13: Gold Nanoparticle – Quantum Dot Based Biosensor¹⁶

3. Cell Adhesion

3.1 Introduction

Agarose is a common brain tissue “phantom” used extensively with neuronal-type cell studies. Cells have been grown and studied in agarose, but modification of the original gel is needed to better support cell growth.⁸ This adjustment has previously been achieved through altering the polymeric backbone of the gel with various peptide fragments that support cell adhesion. Although chemically altering the backbone of various hydrogels and polymers has been successful, the method usually involves a difficult synthesis process and can be expensive and time-consuming. The synthesis techniques are also generally limited to certain types of gels and polymers, so switching to a new gel to study a different class of cell (such as muscle rather than neuronal) would require the development of a new technique to modify the gel. Modifying the gel or polymer backbone also has the potential of altering its original mechanical properties, which may make it unsuitable for some applications. One possible solution to these difficulties is to create nanoparticle-gel composites that have the desired chemical functionality without having to alter the gel or polymer backbone.

Functionalized gold nanoparticles can be used to modify the properties of an existing gel or polymer in the required manner. Most of the potential gels and polymers that could be used are really a fibrous network of polymer “threads” and as such have small pores between these threads. Gold nanoparticles can be added to the gel during the gelling process so that as the gel sets, the particles become entrained in the resulting pores. Gold nanoparticles are ideal for this application because they can be modified with any number of potential organic molecules through a thiol linkage. The chemistry is very simple and involves just mixing the molecule of interest that contains a free thiol group with the gold nanoparticles. This linkage allows the

particles to serve as anchors within the hydrogel for the other molecules, giving the gel new properties because of the attached molecules without changing the chemical structure of the gel itself. Other than this thiol attachment, gold nanoparticles are relatively inert and stable, which makes them excellent “anchors.” The nanoparticles can also be synthesized in different size ranges, making this technique applicable to a variety of gels or polymers with various pore sizes. The same peptides that have previously been used to modify agarose or PEGDA hydrogels for 3-D cell studies can be used to functionalize the gold nanoparticles, giving the modified gel essentially the same new properties but achieved through a simpler, more flexible method. Figure 3.1 shows a diagram of a gold nanoparticle with its supporting ligands and the added functional group ligands. In a modified gel, these nanoparticles and their attached cell adhesion molecules would surround and interact with a growing cell (Figure 3.2).

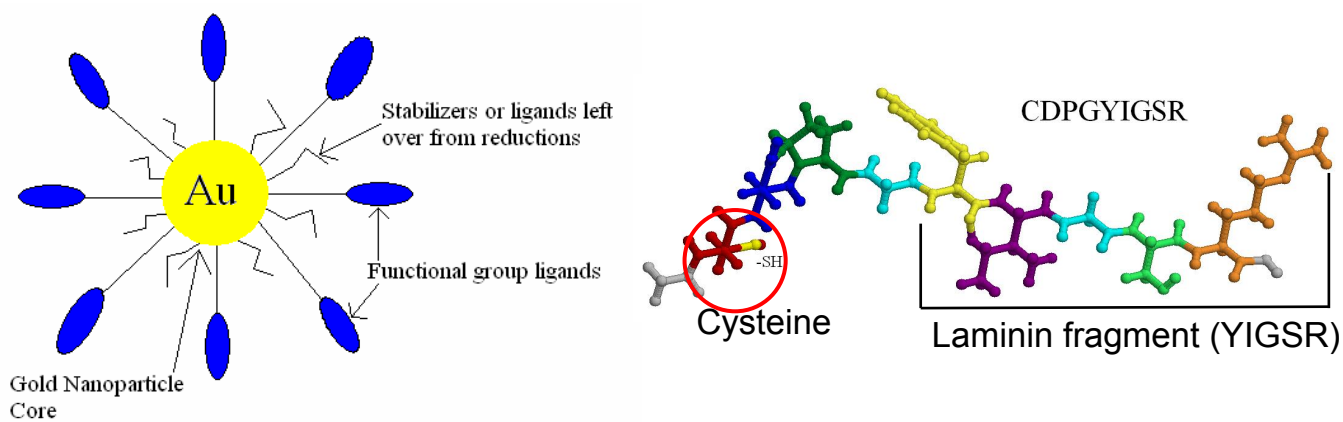


Figure 3.1: Schematic of a Single Functionalized Gold Nanoparticle (left) with the Structure of the Adhesion-Promoting Peptide CDPGYIGSR (right)

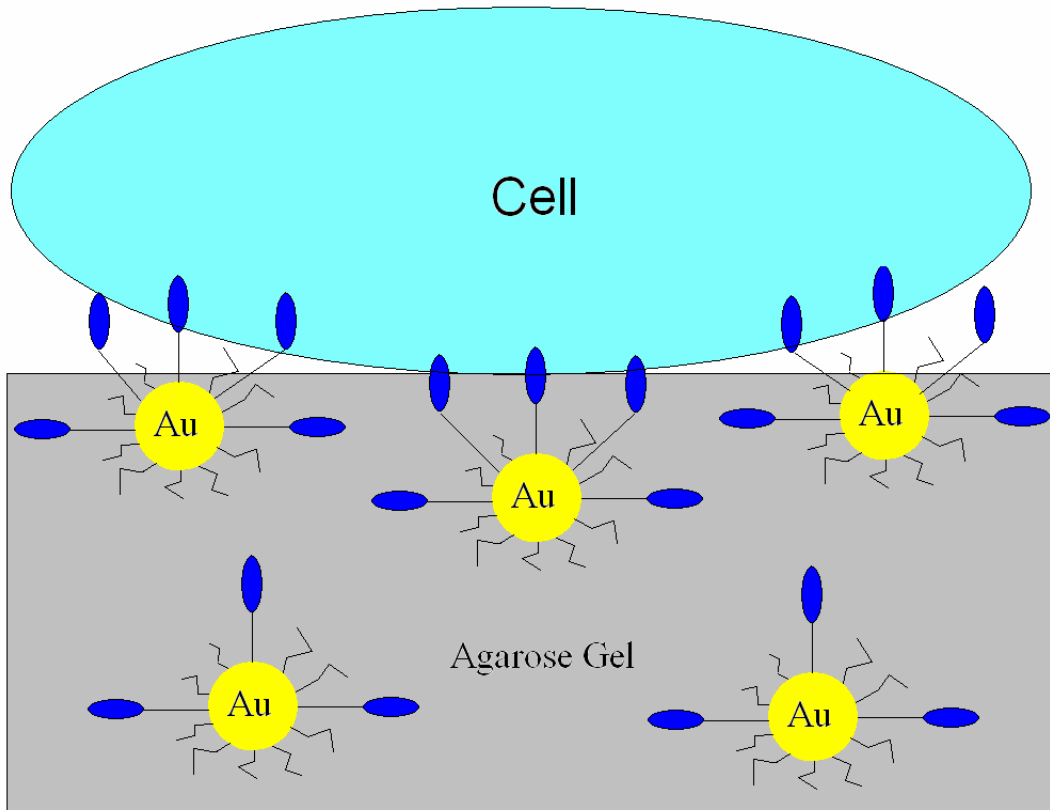


Figure 3.2: Diagram of a Gold Nanoparticle Composite Hydrogel Interacting with a Nearby Cell (not to scale)

In order to test the effectiveness of the proposed technique, a case using PC12 cells (neural progenitor cells that express a neural phenotype with exposure to nerve growth factor) and agarose hydrogels was first considered. Gold nanoparticles of the desired size range were synthesized and characterized via absorbance, dynamic light scattering, and scanning electron microscopy. Gold nanoparticles were then entrained in agarose hydrogels, and the particle elution and mechanical properties of the composite gel were tested. Cell adhesion studies were then performed on the composite hydrogels. Additional cell adhesion tests were also performed with composite PEGDA hydrogels in addition to agarose gels.

3.2 Experimental

3.2.1 Gold Nanoparticle Synthesis

Due to the 80-90 nm pore size of agarose, gold nanoparticles of 90-100 nm were required to provide the greatest chance of remaining entrained in the hydrogel structure over time.

Nanoparticles of this size range are available from commercial sources (Ted Pella, Nanopartz Gold Nanoparticles, etc.), but may also be synthesized by several laboratory methods. A simple temperature controlled synthesis method was examined here for the production of approximately 90 – 100 nm gold nanoparticles.¹² In this reaction, increased temperature results in a decrease in particle size. Spherical gold nanoparticles with diameters of approximately 100 nm were reported using a reaction temperature of 20°C, while a mixture of geometries, including spherical, square, triangular, and hexagonal nanoparticles, with roughly 20 nm diameters were created using a reaction temperature of 100°C. In a modification of the procedure developed by Song *et al*, a stock solution of 0.01 M HAuCl₄ was first created by dissolving HAuCl₄·H₂O [Sigma Aldrich 254169] in Millipore purified water. 80 μL of this stock solution were added to 4.92 mL of Millipore purified water to create 5.0 mL of 1.6x10⁻⁴ M HAuCl₄. This solution was allowed to equilibrate to 19°C in a controlled temperature bath. 200 μL of 2.08 N,N-dimethylacetoacetamide (DMAA), diluted from a solution of 80% DMAA [Sigma Aldrich 537373] using Millipore purified water, were then added to the HAuCl₄ under vigorous stirring. The mixture was mixed for 10 minutes and then allowed to sit for an hour, all while maintaining the solution temperature at 19°C. Nanoparticle solutions were stored at 4°C in a dark glass vial and were found to be stable for approximately one week after synthesis without further modification. All glassware used in the reaction was pre-treated with aqua regia to dissolve any impurities that may interfere with the nanoparticle synthesis.

3.2.2 Gold Nanoparticle Characterization

The nanoparticles were characterized immediately after the synthesis reaction was completed by determining their absorbance using a Genesys 6 [Thermo Electron Corp.] UV-vis spectrophotometer. The sample was also analyzed using dynamic light scattering and scanning electron microscopy. A commercial sample of 90 nm gold nanoparticles from Nanopartz Gold Nanoparticles was also acquired and tested in the same manner for comparison.

3.2.3 Gold Nanoparticle – Hydrogel Composite Creation

A 3.0 wt % solution of Seaprep agarose [Lonza] (commonly used for cell studies because of its lower gelling temperature and clear color) was prepared by slowly dissolving the appropriate amount of Seaprep powder in a stirred solution of phosphate buffered saline (PBS) [Sigma Aldrich P3813]. (For example, 0.15 g of Seaprep powder in 5.0 mL of PBS, neglecting the small volume of the Seaprep powder, makes a 3.0 wt % solution). The solution was weighed and then stirred and heated to boiling where it was maintained for at least 20 minutes until all of the Seaprep had dissolved. The solution was reweighed and more PBS added to correct for evaporation. An equal volume of gold nanoparticle solution (at its synthesized concentration) was then added to the Seaprep solution so that it would be diluted by half, to a final concentration of 1.5 wt %. The gel was then poured into the desired molds and stored at 4° C for 2.5 hours to gel before being removed from the molds (if necessary) and stored under PBS. Gels were made with both Nanopartz 90 nm gold nanoparticles as well as the DMAA synthesized nanoparticles; however, the Nanopartz composite gels were used for most of the subsequent tests due to their stronger optical absorbance and greater stability over time.

Control gels with no nanoparticles were made by diluting the starting 3% solution with PBS to best simulate the process involved in making the nanoparticle composite gels. 1.0% and 2.0% composite gels were made as well by diluting the 3% gel solution with the appropriate amount of nanoparticle solution or PBS. However, to keep the particle concentration the same in each gel type, the nanoparticle solution was either concentrated or diluted with PBS before mixing. The solutions were concentrated by centrifuging them at 10,000 RPM's for 3-5 minutes at 20°C until the particles were all collected into a pellet at the bottom of the centrifuge tube. The appropriate volume of solution was removed, and the particles were resuspended by thoroughly vortexing the solution. This technique was also used to create nanoparticle solutions that were five (5x) and ten times (10x) the original concentration (1x = $\sim 2.65 \times 10^9$ nanoparticles/mL, as calculated based on the original solution concentration given in the Nanopartz product literature¹⁴). These increased concentrations were used to create composite gels as previously described. The 1.5% gels were made with a 1:1 volume ratio of 3% Seaprep agarose and nanoparticle solution of the chosen concentration. The nanoparticle solutions for the 1.0 and 2.0% gels were appropriately concentrated or diluted as before so that the same number of particles would be present in each type of gel to match the amount in the corresponding concentration level (0x, 1x, 5x, or 10x) in the 1.5% gels.

3.2.4 Elution Tests

An elution study was performed to determine if the gold nanoparticles were remaining entrained within the composite gels over time. Nanopartz 90 nm and Seaprep agarose composite hydrogels were created as previously described in gel concentrations of 1.0, 1.5, and 2.0 wt % with each gel type containing gold nanoparticles at the 0x, 1x, 5x, and 10x concentration levels. At least three gels of each possible combination were made in a 96 well plate. 100 μ L of each gel

were added to the wells, and the remaining 200 μL was composed of PBS solution. The absorbance of each well was measured with a Versa Max UV-vis plate reader [Molecular Devices] at 563 nm, the absorbance peak for the Nanopartz 90 nm sample. The gold nanoparticle – free gels were used as “blanks” so that the absorbance of the nanoparticles alone could be measured. The absorbance readings for the samples of each type were averaged together to obtain a single value for that sample type. Readings were taken every 30 minutes initially, and then the time interval was extended to several hours. Sampling continued for four days. Before each measurement, the PBS solution above each of the gels was replaced to provide a fresh concentration gradient for particle diffusion. Figure 3.3 provides a rough sketch of the well-plate setup.

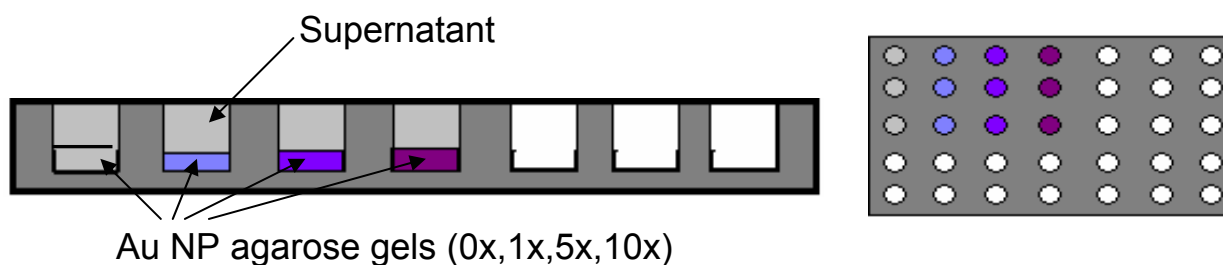


Figure 3.3: Gold Nanoparticle Elution Experiment Sketch (left – profile view of well plate; right – top view of well plate with one gel concentration set of samples shown)

3.2.5 Rheological Tests

Nanopartz 90 nm and 1.5% Seaprep agarose composite hydrogels with 0x, 1x, 5x, and 10x gold nanoparticle concentrations were prepared as previously described using circular perfusion chambers [Grace Bio Labs – PC1R] as molds. Once the gels were solidified, they were removed from the chambers and stored under PBS for a day to allow enough time for them to swell to their equilibrium state. They were then tested on a MCR 300 plate rheometer [Physica]. The gels were maintained at a temperature of 24°C via a Peltier plate while testing using a gap height of

1.5 mm. An amplitude sweep was performed first to determine the optimal strain. A frequency sweep was then performed at the optimal strain value to determine the storage modulus (G') and loss modulus (G'') at each frequency. Figure 3.4 provides a sketch of the rheometer operation, where the lower Peltier plate is fixed and the upper plate oscillates while compressing the gel between the two plates. The rheometer measures the associated resistance to motion as the upper plate oscillates in order to calculate the relevant parameters.

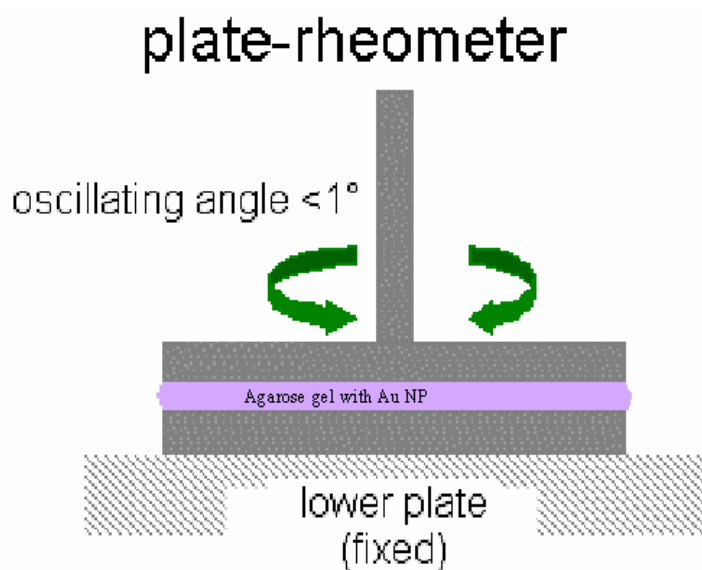


Figure 3.4: Rheometer Setup with Hydrogel Sample

3.2.6 Cell Studies

3.2.6.1 Preparing Sterile Agarose Gels

3.0 wt % sterile Seaprep agarose [Lonza] gels were prepared in a similar manner to that described in Section 3.2.3. Since the gels were to be used for cell adhesion studies, they were prepared in Dulbecco's phosphate buffered saline (D-PBS) [Sigma Aldrich D5773] rather than PBS so as to encourage cell adhesion because of the added calcium and magnesium ions. Gel preparation steps (and all subsequent cell study tests) were performed with sterilized instruments

in a sterile tissue culture hood whenever possible. After the solid agarose had fully dissolved, the gel solutions were autoclaved for 5 minutes. (The gel can potentially lose strength when exposed to longer autoclave cycles.¹⁷) The gel solution was then aliquoted in 0.5 mL increments into sterile microfuge tubes and centrifuged for 1 min at 10,000 rpm's to remove air pockets. The microfuge tubes were gelled at 4°C for 2 hours and then placed under UV light for 20 minutes to ensure sterilization. The gel samples were stored at 4°C until they were needed.

3.2.6.2 Preparing Sterile Composite Gels for Cell Adhesion Tests

In preparation for the creation of the test gels, 30 μ L aliquots of 10 mg/mL of the cell adhesion peptide Ac-CDPGYIGSR (MW 1009.12, 90% pure) [GenScript] were prepared and frozen until needed, and a solution of Nanopartz 90 nm gold nanoparticles was sterile syringe filtered using a filter with a 0.22 μ M pore size and stored for later use. For each test to be performed, five microfuge tube aliquots of the sterilized 3.0 wt % agarose were placed in a 75° C water bath until melted. Five samples were made by modifying the 3.0 wt % gels with additional solutions to create five composite gels, as illustrated in Figure 3.5. For the negative and positive controls, 0.5 mL of sterile D-PBS was added to the corresponding microfuge tube for each sample. The microfuge tubes were vortexed briefly and allowed to re-equilibrate to 75° C in the water bath. At this point the tubes were vortexed and agitated until the gel solution was thoroughly mixed and homogenous. The experimental sample was prepared by thawing and adding one of the previously prepared aliquots of the Ac-CDPGYIGSR peptide to 1.0 mL of sterile filtered gold nanoparticles. The solution was vortexed thoroughly to mix and allowed to sit for 5 minutes to react. 0.5 mL of the gold nanoparticle-peptide solution was then added to an agarose aliquot in the same manner as the controls. Two additional samples, a gold nanoparticle only and a peptide only sample, were also prepared. For the gold nanoparticle sample, 0.5 mL of

sterile filtered gold nanoparticles was added to an agarose gel microfuge tube. For the peptide only sample, an aliquot of Ac-CDPGYIGSR peptide was added to 1.0 mL of sterile D-PBS and vortexed well to mix. 0.5 mL of the combined solution was then added to the agarose gel microfuge tube in the same manner as the other samples.

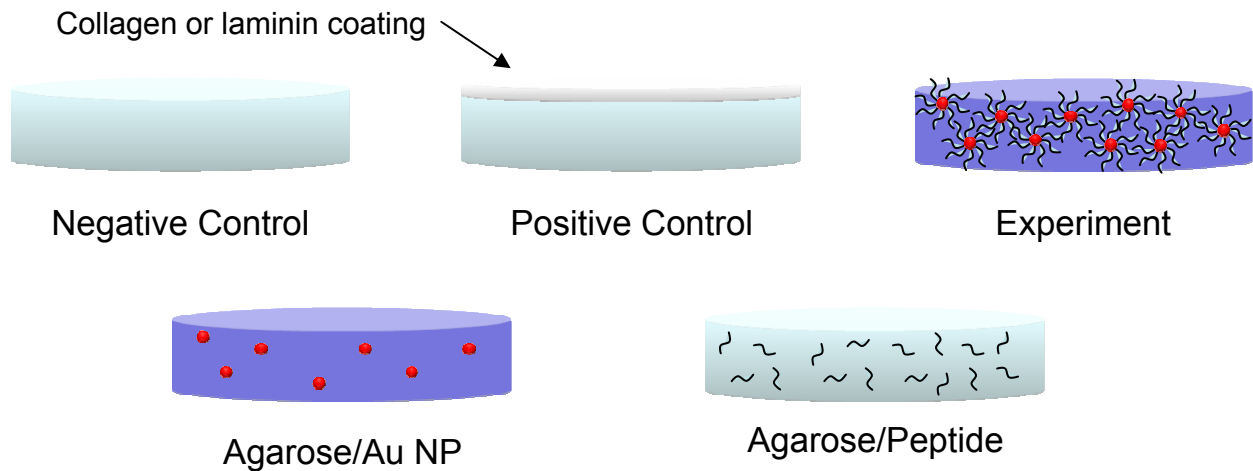


Figure 3.5: Gels Created for Cell Adhesion Pilot Experiments

After each gel solution was prepared, they were added to circular perfusion chambers [Grace Bio Labs – PC1R] which served as molds and stored at 4°C for two hours until they were fully gelled. The gels were then carefully transferred to a 6 well plate with the wells containing sterile D-PBS solution. The gels were allowed to sit in solution for two hours in order for any swelling or size change to take place. The D-PBS solution surrounding each gel was then carefully exchanged with fresh solution to allow for the removal of any loose particles that may have come off from the gel surface. Instead of immediately replacing the solution surrounding the positive control with fresh D-PBS, a 50 µg/mL solution of collagen (Type 1, rat tail) [BD Biosciences 354236] in 0.02 N acetic acid was instead added to the well so that the gel surface was covered. The well plate was allowed to sit at room temperature for an hour to allow the collagen time to

form a thin layer across the agarose gel surface. The collagen solution was then removed and the gel rinsed twice with fresh, sterile D-PBS to remove traces of the acetic acid. The prepared gels were either used immediately after this or stored at 4°C until needed.

3.2.6.3 Culturing Cells on the Composite Gels

Once ready for the cell adhesion experiments to begin, the D-PBS solution around each gel sample was carefully removed and replaced with a culture of PC12 cells (without the addition of nerve growth factor for these early tests) seeded at a density of 2×10^5 cells/cm². The samples were then incubated at 37°C for 24 hours. Phase contrast images of the samples were taken with an Olympus IX71 microscope before further modification of the cells took place. The medium was then carefully removed from each well and each sample washed twice with 37°C sterile D-PBS. The surface of each gel was then covered with a combined solution of 2.0 μM Calcein AM and 1.0 μM EthD-1, created from the LIVE/DEAD[®] Viability/Cytotoxicity Kit [Invitrogen L3224] and incubated at 37°C for 30 minutes before washing the gels twice with 37°C sterile D-PBS. The samples were again imaged with the Olympus IX71 microscope using the appropriate fluorescent filters for the LIVE/DEAD stain. Figure 3.6 briefly illustrates these experiments.

3.2.6.4 Cell Adhesion Experiment Modifications

Experiments were also performed using a modification of the procedure described in the previous section. In this case the gels were formed in trans-well inserts [Fisher Scientific 08-770] designed for 24 well plates instead of in larger separate molds. The same general procedures as before were followed with the exception of the rinsing steps. In this case, the transwell inserts were carefully removed from their original well and transferred to a new well filled with fresh, sterile D-PBS. The solution in the insert was allowed to mix with the fresh solution in the outer well to dilute the portion of solution remaining in the insert. Multiple transfers were performed as

necessary to fully dilute the starting solution as desired. This technique was used to avoid turbulent mixing within the insert and to avoid using micropipets as much as possible due to the shear stress exerted on the cells and the weak agarose gels.

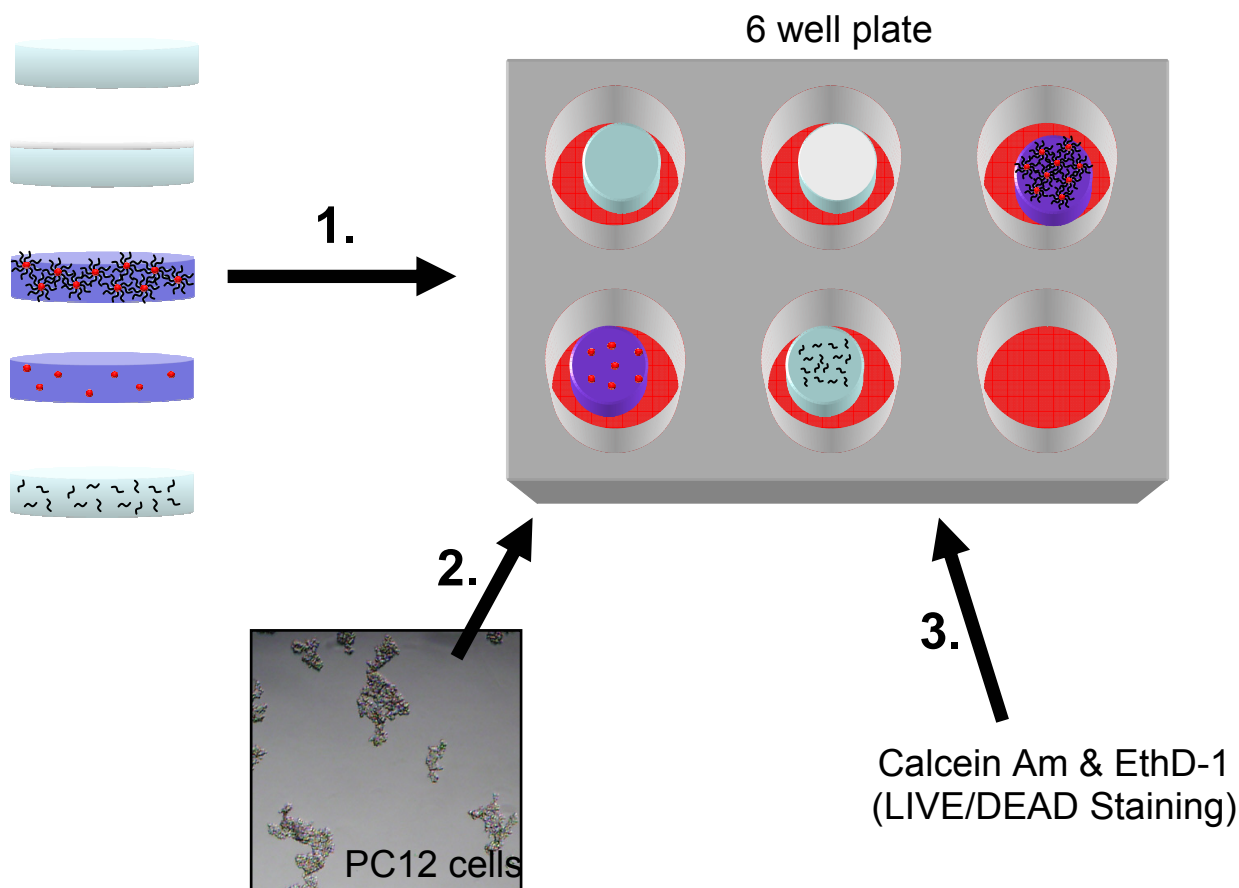


Figure 3.6: Experimental Setup for Initial Cell Adhesion Experiments

3.2.6.5 PEGDA Cell Adhesion Experiments

Initiator solution for the Poly(ethylene glycol) diacrylate (PEGDA) photopolymerization was prepared by adding 0.333 g of Irgacure 2959 [Ciba] to a microfuge tube followed by 1 mL of N-Vinyl-2-pyrrolidone (NVP) [Sigma V3409]. The solution was vortexed until homogenous and stored at room temperature in the dark until needed. The initiator solution and a solution of 15 nm gold nanoparticles [Ted Pella 15704] were sterile filtered using a 0.22 μm filter. A covered

balance was sprayed down with 70% ethanol to form a pseudo-sterile environment where 0.22 g of 1000 MW PEGDA [Laysan Bio] was added each to five sterile microfuge tubes. For the negative and positive controls, 1 mL of sterile D-PBS was added to one of the PEGDA microfuge tubes and the solution vortexed thoroughly. A 30 μ L aliquot of CDPGYIGSR peptide was added to 1 mL of sterile-filtered 15 nm gold nanoparticles, vortexed thoroughly, and transferred to a PEGDA microfuge tube to form the experimental solution. For the gold only solution, 1 mL of sterile 15 nm gold nanoparticles was added to a PEGDA microfuge tube. The peptide only solution was prepared in the same fashion as the experimental solution except 1 mL of sterile D-PBS was used instead of the gold nanoparticle solution. After each of the PEGDA solutions was mixed until homogenous, 10 μ L of the sterile initiator solution was added to each sample. The solutions were then mixed again and added to the desired well plate or gel mold before being placed under a UV lamp for 10 minutes for polymerization to take place. After the gels had been polymerized, they were treated in the same fashion as the agarose gels as previously described (rinsing, collagen coating, seeding cells, etc.). The PEGDA gels, however, were more robust than the agarose gels and could be washed using pipets without damaging the gel surface if desired.

3.3 Results and Discussion

3.3.1 Gold Nanoparticle Characterization

The absorbance spectrums of the gold nanoparticles synthesized using the modified N,N-dimethylacetamide reduction are shown below in Figure 3.7. The DMAA synthesized nanoparticles had an absorbance peak of approximately 569 nm, and the commercial 90 nm Nanopartz gold nanoparticles had their peak at 563 nm. The close proximity of these values provides a preliminary indication of a similarity in size of the two types of particles, with the DMAA particles potentially being slightly larger due to the longer absorbance wavelength. However, the peak absorbance of the DMAA synthesized particles is lower than that of the commercial sample, indicating that the synthesized particles are lower in concentration.

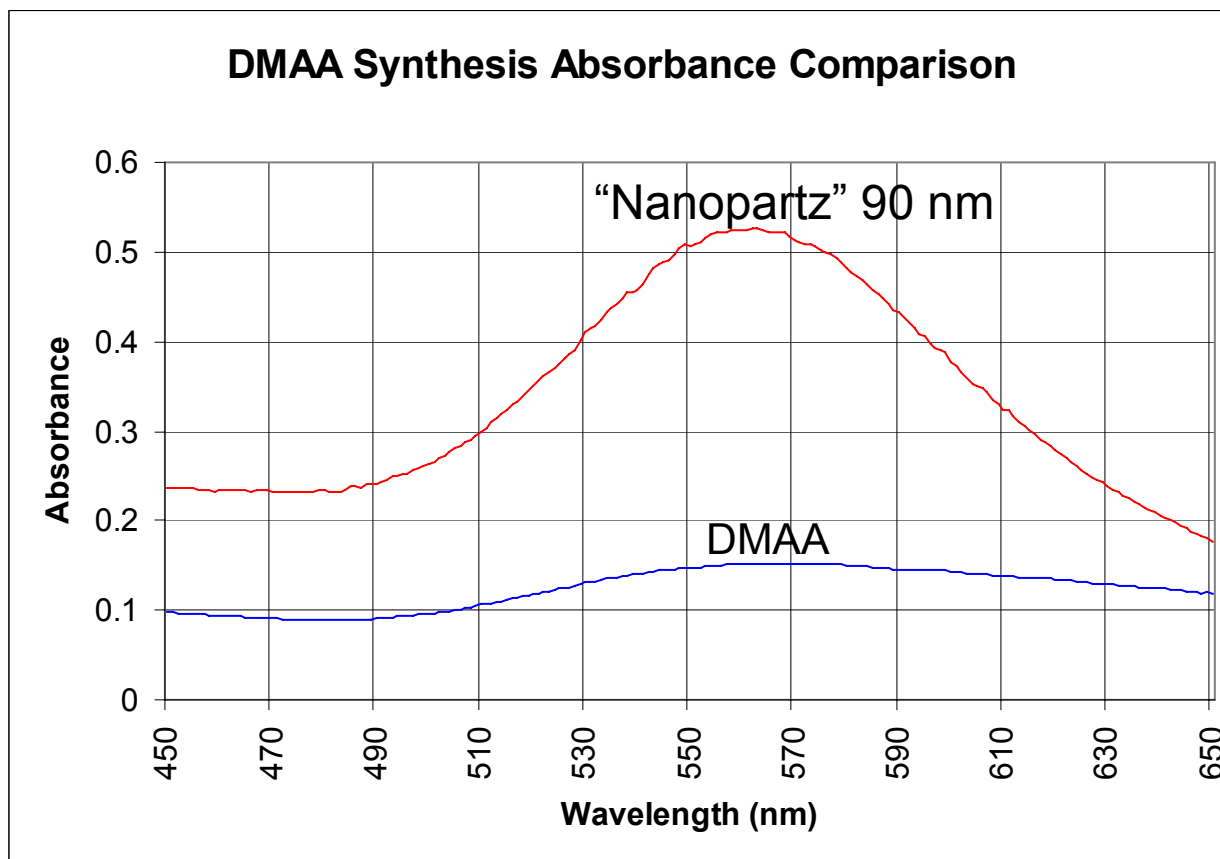


Figure 3.7: Absorbance Spectrums of DMAA synthesized and Commercial 90 nm Gold Nanoparticles

Figures 3.8 and 3.9 compare the dynamic light scattering (DLS) results for the synthesized and commercial gold nanoparticles. The intensity of the peak is higher for the commercial sample, again indicating its higher concentration. The peak for the commercial sample specifies a particle diameter slightly larger than 100 nm, but since DLS measures the hydrodynamic radius of the particles, some size inflation is expected. The DMAA sample has a peak particle size at a smaller diameter than the commercial sample, but the size distribution is wider and bimodal with a small tail. This tail indicates the presence of a small amount of much smaller nanoparticles in the synthesized sample. While these smaller particles are less desirable, they do not make up the bulk of the sample and will not interfere with the planned application. The wider primary peak in the synthesized sample indicates that they are less monodisperse than the commercial counterparts. The SEM images in Figure 3.10 confirm this, but overall the two samples appear very similar, and the non-spherical shapes of some of the synthesized particles may actually help contain them within the polymer network once embedded.

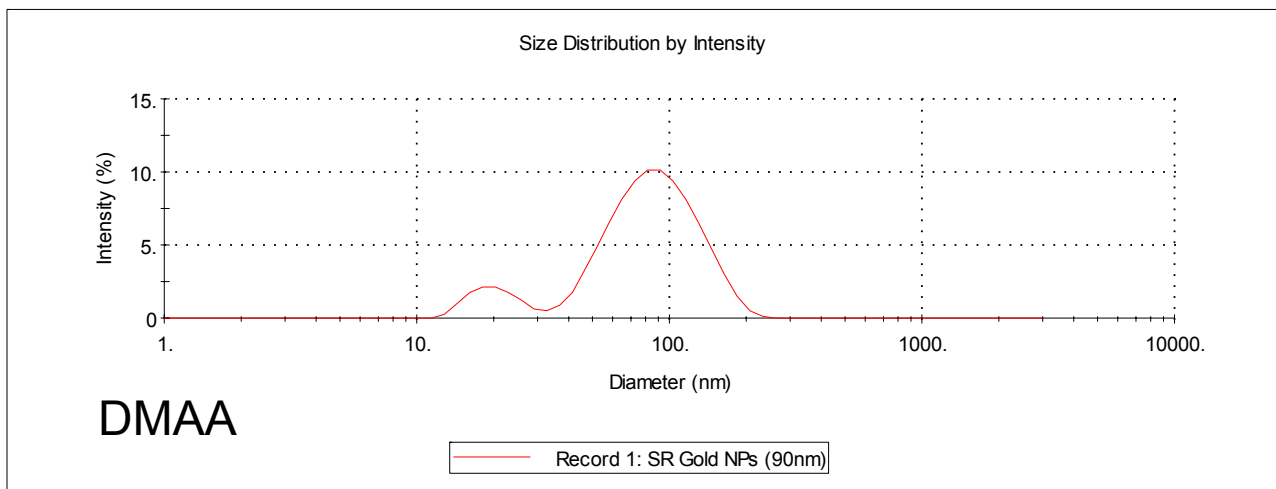


Figure 3.8: DMAA Gold Nanoparticles Dynamic Light Scattering Results

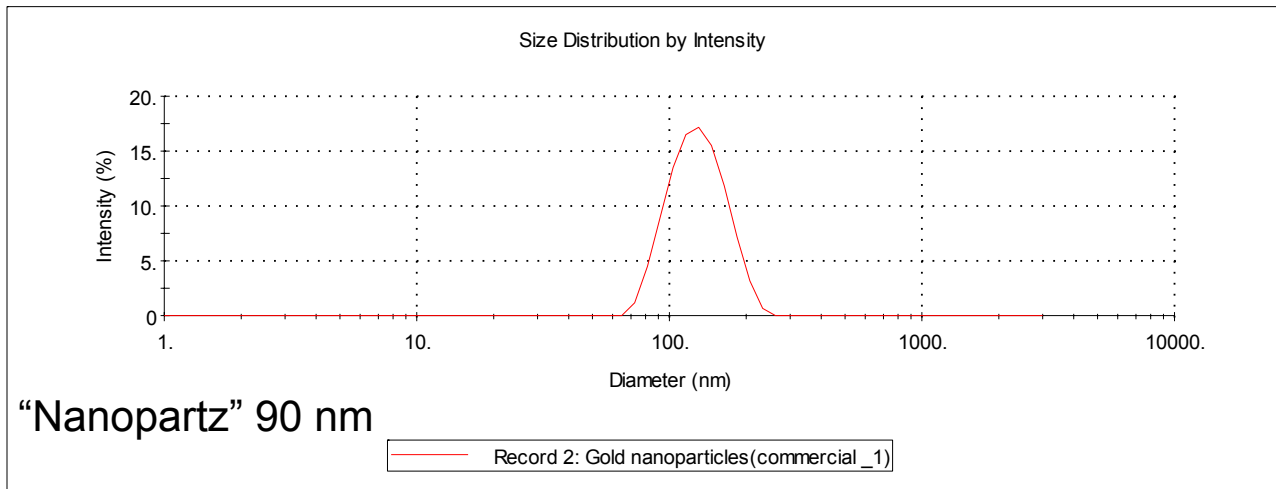


Figure 3.9: “Nanopartz” 90 nm Gold Nanoparticles Dynamic Light Scattering Results

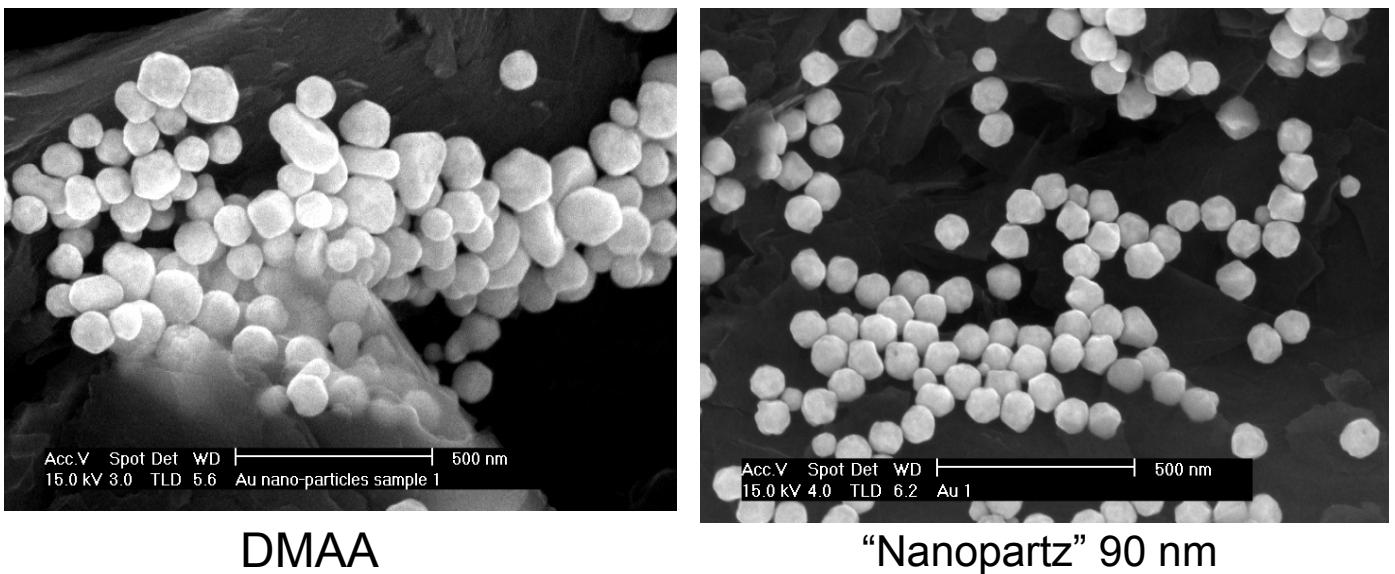


Figure 3.10: SEM Comparison of DMAA and “Nanopartz” 90 nm Gold Nanoparticles

Based on these measurements, the DMAA synthesized particles are close enough in size and shape to the commercial comparison sample to be a valid substitute. The commercial samples are very monodisperse and eliminate the necessity of synthesizing particles for use in the gold-polymer composites, but the exact surface chemistry is proprietary. If complete control over this surface chemistry becomes necessary in future applications, laboratory synthesized particles will

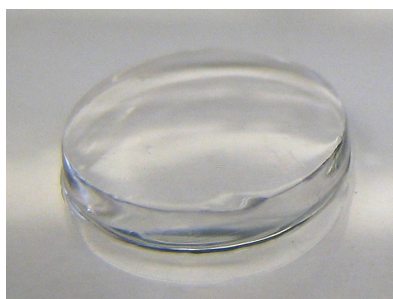
be required. The DMAA synthesis is a favorable technique for this application, since the size of the synthesized particles can be tuned simply by changing the reaction temperature.

3.3.2 Gold Nanoparticle – Hydrogel Composites

Adding the gold nanoparticle solution to the Seaprep agarose and thoroughly mixing before the gel was cooled resulted in a final uniform hydrogel of the same distinct color as the original solution. No ill effects such as particle aggregation were observed for the composite gels, and mixing the particles into the higher temperature gel didn't create any complications. Figures 3.11 and 3.12 show examples of two different sizes of composite hydrogels formed using the previously described techniques. As expected, the color of the gel becomes increasingly darker as the nanoparticle concentration increases.

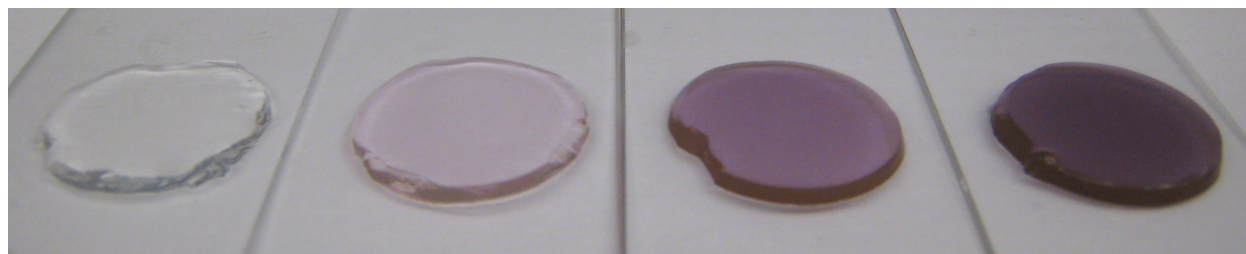


Nanopartz 90 nm gold nanoparticles
in 1.5 % Seaprep agarose



1.5% Seaprep Agarose

Figure 3.11: Comparison of Modified and Unmodified Agarose Hydrogels



0x

1x

5x

10x

$\sim 2.65 \times 10^9$ NP's/ mL

$\sim 13.3 \times 10^9$ NP's/ mL

$\sim 26.5 \times 10^9$ NP's/ mL

Figure 3.12: Seaprep Agarose Hydrogels with Increasing Gold Nanoparticle Concentration

3.3.3 Elution Test Results

Figure 3.13 below includes the data for each sample of the elution test. Samples of 1.0, 1.5, and 2.0 wt % Seaprep agarose at 1x ($\sim 2.65 \times 10^9$ NP's/ mL), 5x ($\sim 13.3 \times 10^9$ NP's/ mL), and 10x ($\sim 26.5 \times 10^9$ NP's/ mL) concentrations of Nanopartz 90 nm gold nanoparticles were tested. Although the samples of each 1x, 5x, or 10x type contained the same amount of nanoparticles, the extremely viscous nature of the concentrated agarose solutions made measuring them difficult, creating small variations in the actual agarose concentration of the final gel types. These variations meant that the initial absorbance of the gels for each nanoparticle concentration type would vary slightly. While this is the case, the overall trend for each sample is to maintain approximately the same absorbance but with a slight decrease over time. Some decrease is expected as not all of the particles will be as tightly bound within the pore structure as others, and portions of the top layers of the gels can even be removed during the solution exchange steps due to the weak nature of the agarose hydrogels. The hydrogels can also swell slightly over time, diluting the sample to a small degree. As expected, the samples with higher nanoparticle concentrations had higher absorbances, and these absorbances were in ratios approximately the same as the concentrations. One interesting observation is that the 1.0% samples break the general trend, and their absorbances actually increase over time. Since the 1.0% samples are the least concentrated, they will have larger pores than the other samples, potentially enabling the nanoparticles to interact more with each other and begin to aggregate slightly, increasing the absorbance intensity. This aggregation occurs normally over time in solutions of 90 nm Nanopartz gold nanoparticles, but the particles can be resuspended upon vortexing. Despite the slight variations, the majority of the nanoparticles are clearly remaining entrained within the pore structure of the gel over time. This is true for a range of agarose and nanoparticle concentrations.

Figure 3.14 also demonstrates that gels that spend an extended amount of time in large volumes of solution retain the distinctive color of the embedded gold nanoparticles.

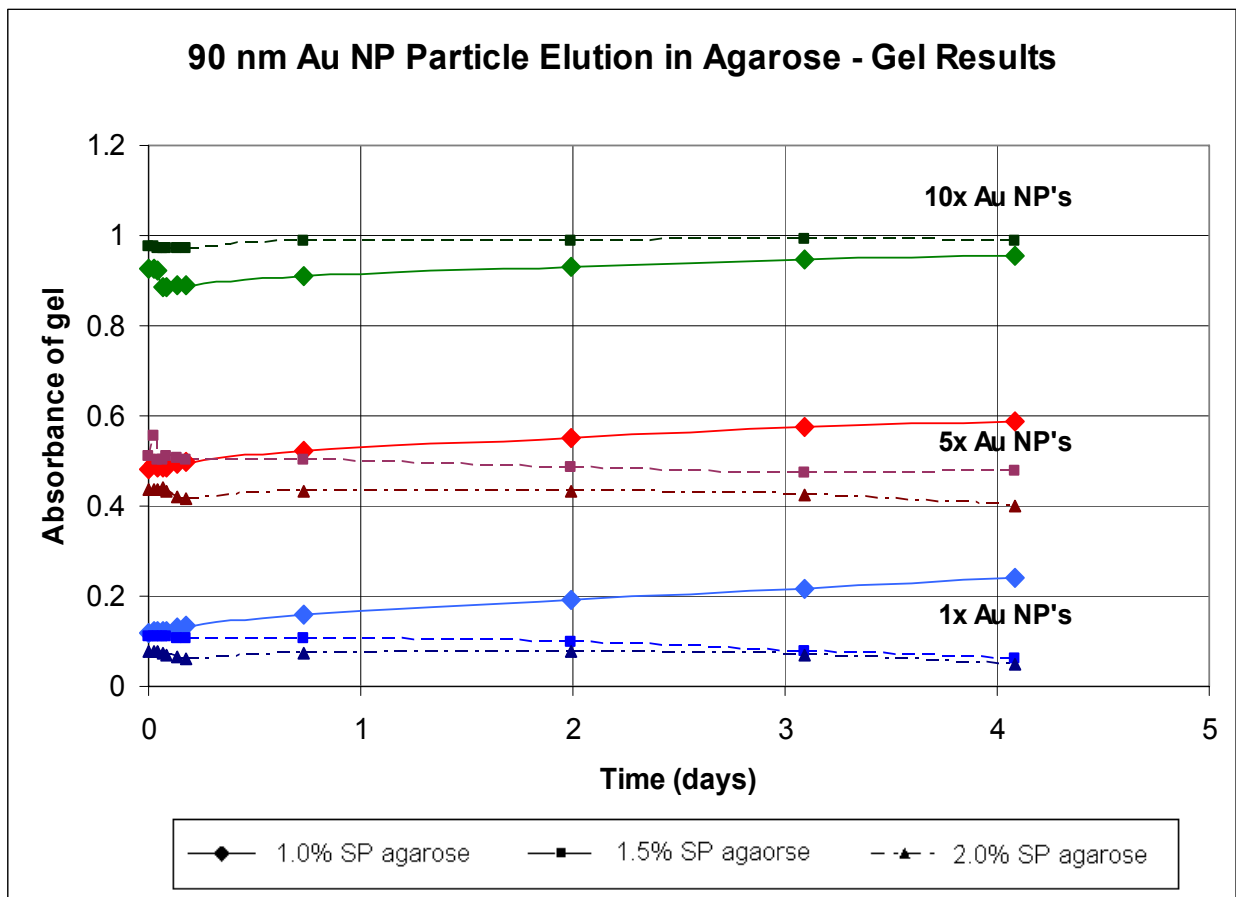


Figure 3.13: Nanopartz 90 nm Particle Elution in Seaprep (SP) Agarose – Gel Absorbance Measurements



Figure 3.14: Composite Seaprep Agarose (1x) Hydrogel after 13 Days in PBS

3.3.4 Rheological Test Results

By compressing the gel samples and measuring the associated resistance to motion with the upper plate of the rheometer, a few key parameters were able to be calculated for the physical properties of the gel, including the storage and loss moduli. The storage modulus (G') represents how solid-like, or elastic, a material is whereas the loss modulus (G'') represents how liquid-like, or viscous, that material is.¹⁸ Combined they make up the shear modulus, which measures the visco-elastic character of the material. Since the strain used for the frequency sweep tests was pre-determined from the amplitude sweeps, the moduli for each gel were nearly constant over the frequency range. The mean and standard deviation of the storage and loss moduli for each sample type were obtained from the average of these values for each of three replicates for each sample and are graphed in Figures 3.15 and 3.16, respectively. If $G' > G''$, the material will have a more solid and consistent but flexible shape. If $G' < G''$, the material will be more liquid-like and will likely leak or run over time. For all samples tested, the storage modulus is greater than the loss modulus, which is expected since although agarose is a very weak material, it does have a set shape and will tear rather than leak if stressed too far.

No consistent trend is seen with either the storage modulus or the loss modulus with increasing concentration of gold nanoparticles in the composite gels. The standard deviations are also very large. Using Student's t-test ($\alpha=0.05$), there is no significant difference within the means of each set of G' and G'' measurements. Based on these tests, 63 samples would be needed to resolve G' and 55 for G'' using a power of 0.90. While additional tests are planned to test the effects of different agarose concentration as well as gold concentration on the rheology of the gels, testing 50 – 60 samples can be considered excessive. The large standard deviation and inconsistent trend observed with this set of tests could indicate that there is more gel-to-gel

variation in the creation of the agarose hydrogels than any change in mechanical properties caused by the presence of the gold nanoparticles. One interesting trend though is that the standard deviations for both the storage and loss moduli decrease with increasing gold nanoparticle concentration, which may imply that the nanoparticles have a stabilizing effect on the hydrogel.

Storage Modulus (G') for Gels of Varying Au Concentration

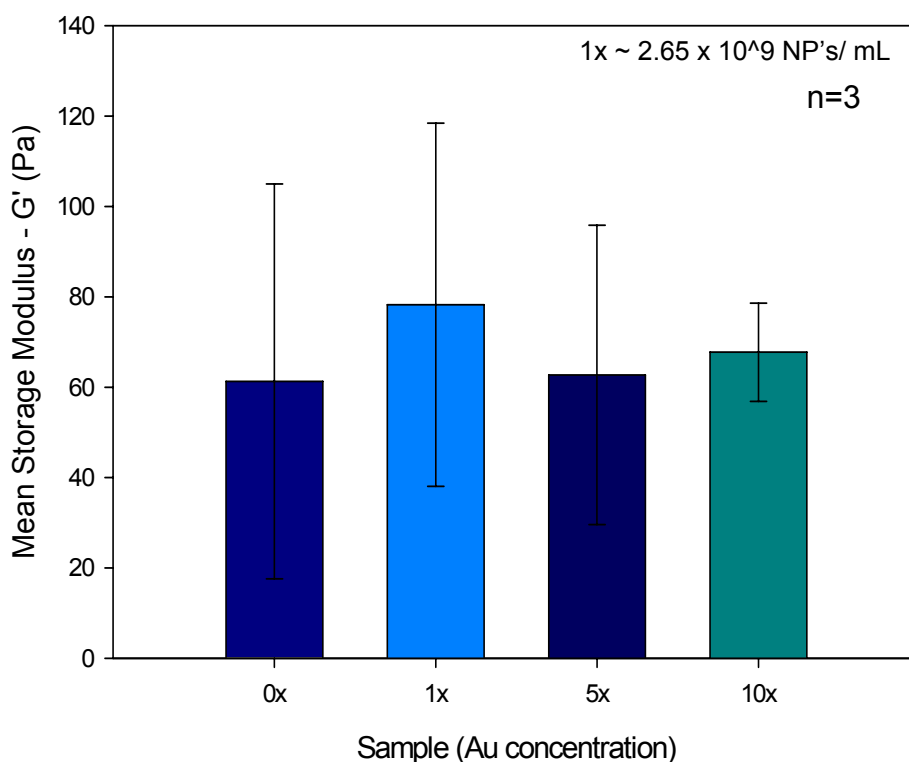


Figure 3.15: Storage Modulus for Composite 1.5% Seaprep Agarose Hydrogels

Loss Modulus (G'') for Gels of Varying Au Concentration

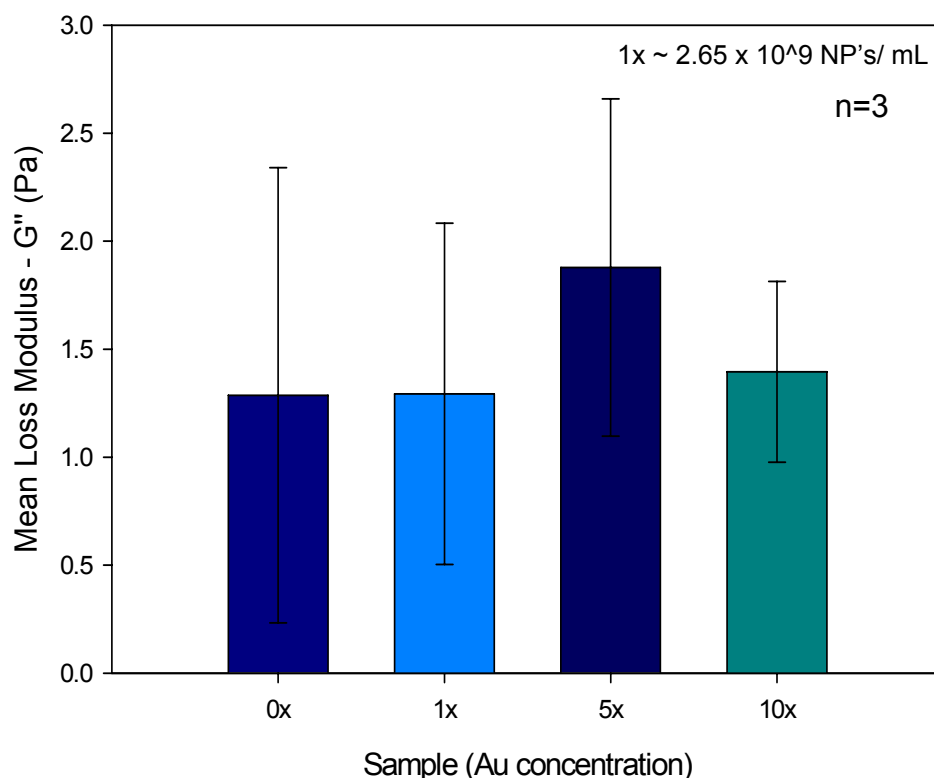


Figure 3.16: Loss Modulus for Composite 1.5% Seaprep Agarose Hydrogels

3.3.5 Cell Studies Results

The gold nanoparticle composite gels made for this experiment were 1.5% agarose with 2.65×10^9 nanoparticles/mL (1x). Approximately 3.4×10^7 peptide molecules per gold nanoparticle were available in the experimental solution, and based on a rough estimation of available nanoparticle surface area assuming a perfectly spherical geometry, enough peptide should be present to completely saturate the gold nanoparticles. Upon addition of the peptide, the gold nanoparticle solution becomes slightly lighter in color, indicating that the peptide may be destabilizing the colloid and causing a small degree of aggregation. Solutions left at this stage will show clear signs of aggregation within 24 hours, but solutions that are immediately mixed with the agarose hydrogels maintain their stability as indicated by no further color change. As such, the experimental gels are slightly lighter in shade than the gold nanoparticle only

counterparts, but the difference is not very pronounced. If some of the particles had aggregated to a degree, it would reduce the total number of available particles for interaction with the cells, but since enough nano-sized particles remained to maintain the characteristic color of the solution, there should also be an adequate number for cell interactions.

The PC12 cells used in this study were non-differentiated since this was an initial trial, and a simple test-case was desired. The behavior of the cells with the imaging techniques was confirmed by seeding them in a collagen coated well plate, as seen in Figure 3.17. As the LIVE/DEAD staining indicates, the cells were generally healthy with the vast majority being alive with only a few stray dead cells.

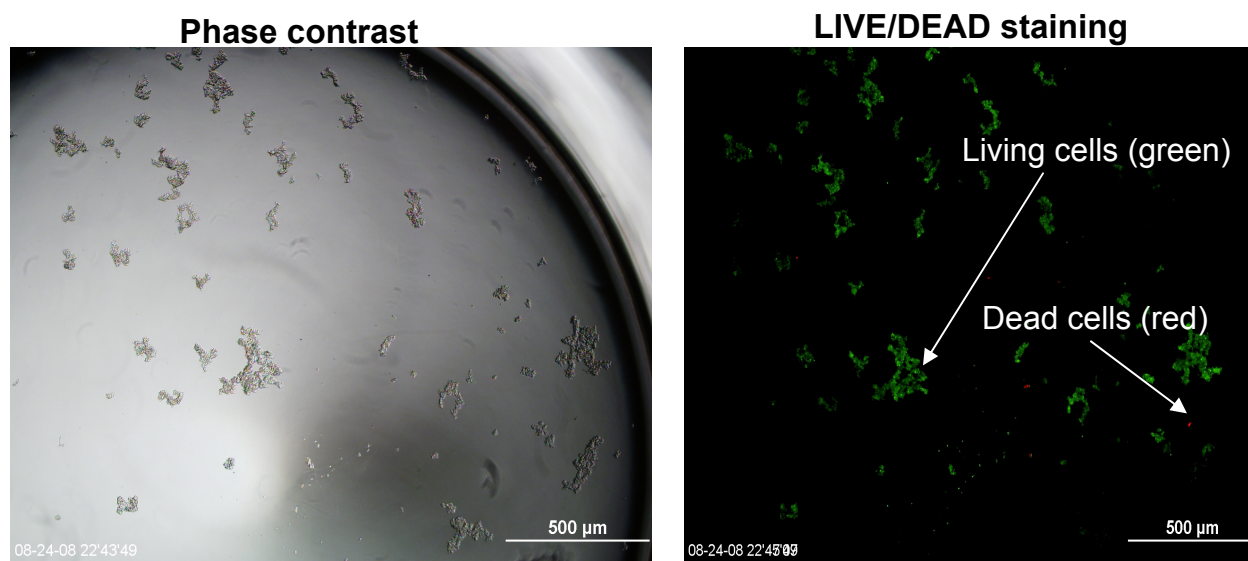


Figure 3.17: Phase Contrast and LIVE/DEAD Staining Images of PC12 cells in a Test Well

The images taken for the 6 well plate experiments are shown in Figure 3.18. The design of this particular experiment was chosen to allow for manipulation of the gels and the ability to perform the rinsing steps without directly interfering with the gel surface due to the extra space around the gels once placed in the 6 well plate (refer to Figure 3.6). However, this extra space (since the wells have a larger diameter than the gels) also prevents a direct numerical comparison

of the number of adherent cells since cells that didn't happen to settle directly over the gels never had an opportunity for adhesion. The number of these cells could potentially be different for each well. What this experiment does offer is the ability to qualitatively analyze the basic growth behavior and appearance of the cells on each sample to determine any large differences in performance. The negative and positive controls appeared similar with a relatively sparsely covered surface featuring some single cells and small clusters. In the images shown the peptide and gold nanoparticle only gels tend to be slightly more heavily covered with some large clusters. The similar nature of the negative and positive controls possibly indicates that the collagen coating on the gel surface did not form or act as intended, since a definite increase in adhesion should be seen with the positive control. The collagen coating on agarose was chosen due to its common use to increase adhesion on culture dishes and ease of formation, but chemically integrating the CDPGYIGSR peptide into the agarose structure as in Bellamkonda's work, while more difficult, would provide a more appropriate positive control comparison to the experimental gels. Subsequent experiments have shown, however, that cells on all of the samples tend to have the same general appearance, although the experimental gels occasionally have some very large clusters of cells present, as indicated in Figure 3.18. In the images shown, these cells were actually observed to have burrowed into the surface of the gel to a degree as indicated by parts of the cluster appearing in different focal planes. Although PC12 cells cannot digest agarose to migrate in this fashion, they can follow existing microfractures within the gel. It is possible that the composite gel would aid in this behavior, but more experimentation is necessary to confirm that this is indeed the case. The LIVE/DEAD staining indicating that this cluster is viable and healthy is encouraging though. Since the number of adherent cells could not be readily compared using the 6 well experiments because of the inherent limitations, and since

none of the gel types exhibit vastly different behavior from the others, a new experimental technique is necessary to quantitatively compare the different gel samples.

Preparing the gels in the trans-well inserts provides an opportunity to address the shortcoming of the 6 well plate experiments. Since the gels cover the whole surface of the insert (essentially a well within a well plate), each cell added has the same chance to reach the gel surface and adhere. The nature of the inserts also allows for easy transfer between the wells of the 24 well plate so that the necessary washing steps can be performed by moving the insert into a well filled with fresh buffer. This allows for diffusion to do most of the mixing and avoid unnecessary stress on the cells or the sensitive agarose gels. A similar technique was examined with forming the gels directly in well plates and rinsing with micropipets, but even with extreme caution, the shear stress from the using the pipets was often enough to remove the cells from the surface of every gel. While this may indicate that the cells are not adhering well at all to any of the samples, the inconsistent nature of the force from the pipet makes this possibility difficult to confirm. In working with the agarose gels and growing cells on the surface, a consistent but weak stress is needed on the sample to provide a better indication of which cells are more adherent, as indicated by the similar nature of the results from the 6 well experiments. The transwell inserts ideally would meet these requirements where the weak stress is applied in the necessary rinsing steps, but there is a drawback to using them. Since the geometry of the inserts is different than the perfusion chamber molds, a deep meniscus is formed in the gel due to the interactions of the gel solution with the walls of the insert. This causes the gel surface to be deeply concave rather than flat. As seen in Figure 3.19, the cells tend to collect in the central concave dip of the gel bonding together into one large mass. The results were the same for each gel type tested. Even careful washing with the inserts as previously described causes the loss of a

majority of the cells, presumably because most are only bound to each other and not the gel surface making them easier to sweep away. In contrast, Figure 3.20 shows cells from the same experiment grown on the transwell insert surface and showing the expected even distribution over the entire surface. The way the cells collect on the gel samples implies that the cells are more adherent to each other than to the gel itself. While this is to be expected for three of the gels (the negative control and the peptide and gold nanoparticle only samples), the positive control and experimental sample should show increased adhesion. Two possibilities for this discrepancy are that the problem is with the samples themselves or that the agarose gel is too far from its ideal mechanical properties and that is negatively affecting the cell adhesion. Future tests with different concentrations of agarose gels could provide more information in this area. One more possibility is that the concavity of the gels is too deep, and the cells are simply funneled to the bottom before any even have a chance to adhere to the gel. Using larger transwell inserts would reduce the meniscus to a degree but would not eliminate it while increasing experimental costs.

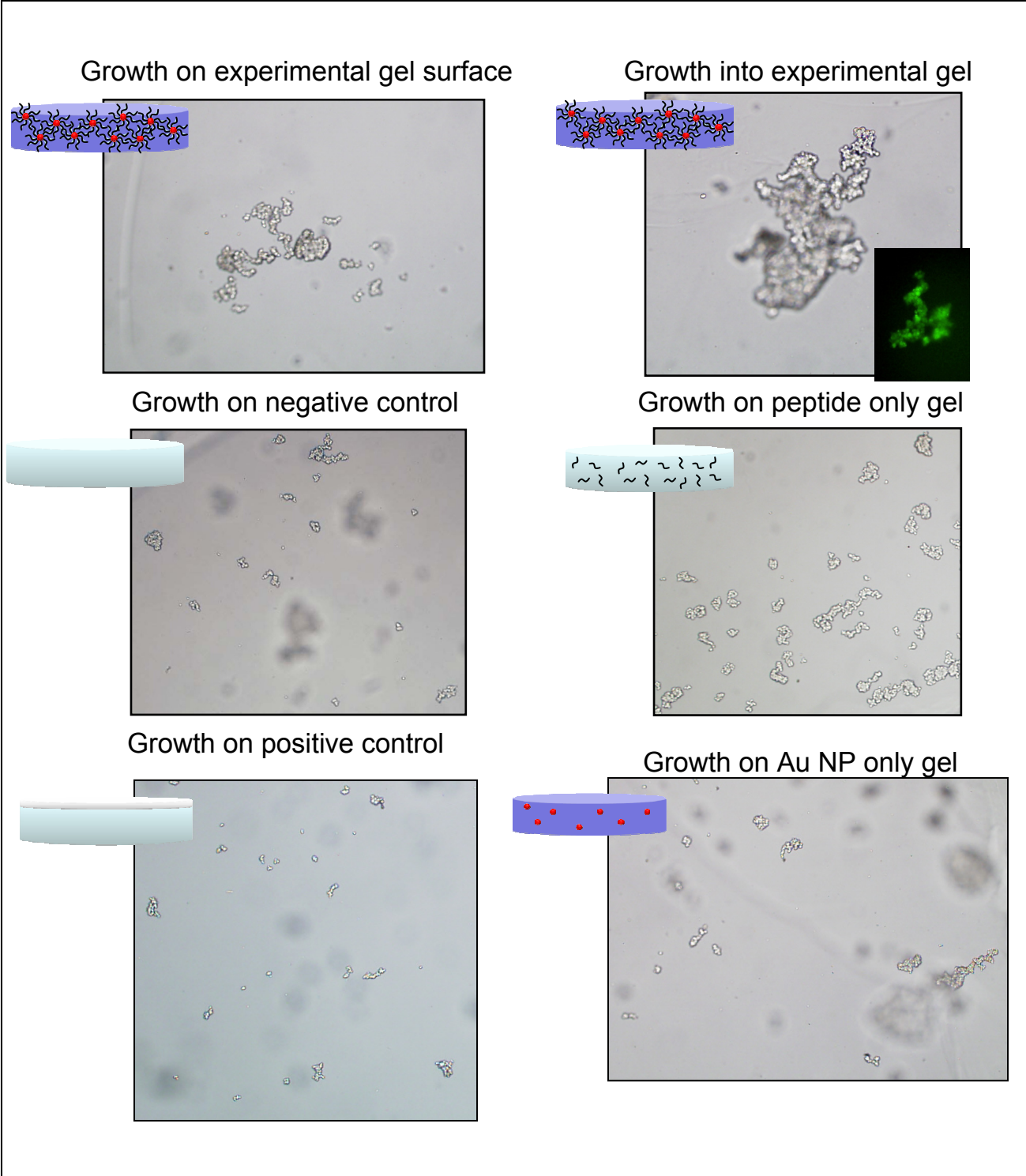


Figure 3.18: 6 Well Plate Experiment Images – 1.5% Agarose (1x Au NP's)

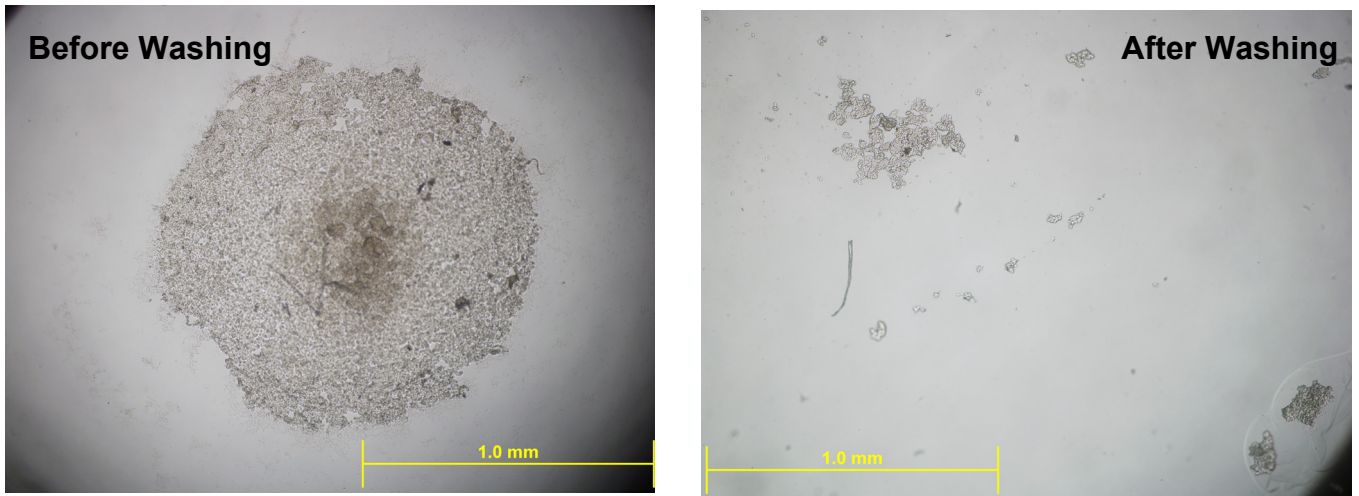


Figure 3.19: Experimental Gel from Transwell Inserts

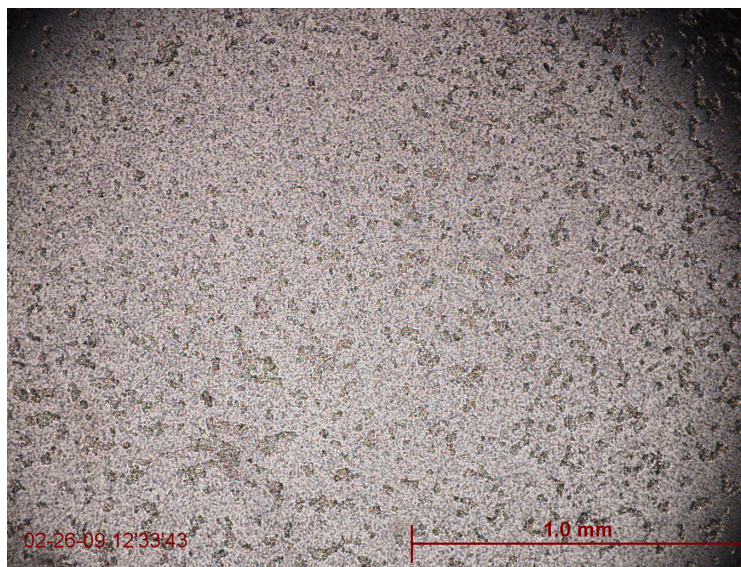


Figure 3.20: PC12 Cells Grown on Transwell Insert Surface

In order to help resolve some of the difficulties experienced with the agarose hydrogels, poly(ethylene glycol) diacrylate (PEGDA) hydrogels were also studied in a similar fashion to determine what difference the base polymer would have on the cells. Similar behavior was seen for all of the samples tested, but as opposed to the agarose tests many of the PEGDA gels had a

large number of adherent cells that were well distributed over the surface. This is shown in Figure 3.21, where some of the gelling was incomplete, creating the depressions in the middle of the samples. The general behavior of the PEGDA gels is the opposite of that of the agarose gels in that the PC12 cells adhered well even to the unmodified gels, indicating the influence of the substrate on adhesion. The PEGDA gels could also be formed directly in well plates and washed with pipets while only losing a small fraction of adherent cells. However, because of the similarity between samples, further quantitative methods are again necessary to determine the effectiveness of the experimental technique, such as through quantifying the extent of fluorescence for each sample while using the LIVE/DEAD stain. Performing this test will also require that the samples be washed and gently stressed in a consistent manner. An interesting behavior was noticed with the current PEGDA tests though. Since the nanoparticles used were 15 nm due to the smaller pore size of the gel, they were observed to be sensitive to the PEGDA solution (before gelling) as well as the CDPGYIGSR peptide itself. The PEGDA alone would shift the color of the nanoparticle solution from a bright red to blue, and the PEGDA with the CDPGYIGSR peptide would yield a purple solution. In the second case, the particles would eventually aggregate into visible clumps if not polymerized. Polymerizing the gels appeared to mostly halt the aggregation, although visible purple deposits were seen in the gel itself. While the gel still had an overall pale purple color, these deposits appeared to be aggregate collections of gold nanoparticles, peptide, and polymer. These are visible in Figure 3.22 where they can be distinctly seen against the rest of the gel which, although light purple colored, appears clear through the microscope. Interestingly, the cells appear to be clustered around the purple nanoparticle deposits to a degree. The presence of the deposits may indicate that the surrounding area could be in the initial stages of aggregation, which may be promoting the adhesion response

of the cells. However, more testing is necessary to determine if this is the case or if some feature of the gel that led to the formation of the deposit in this area is also affecting cell adhesion.

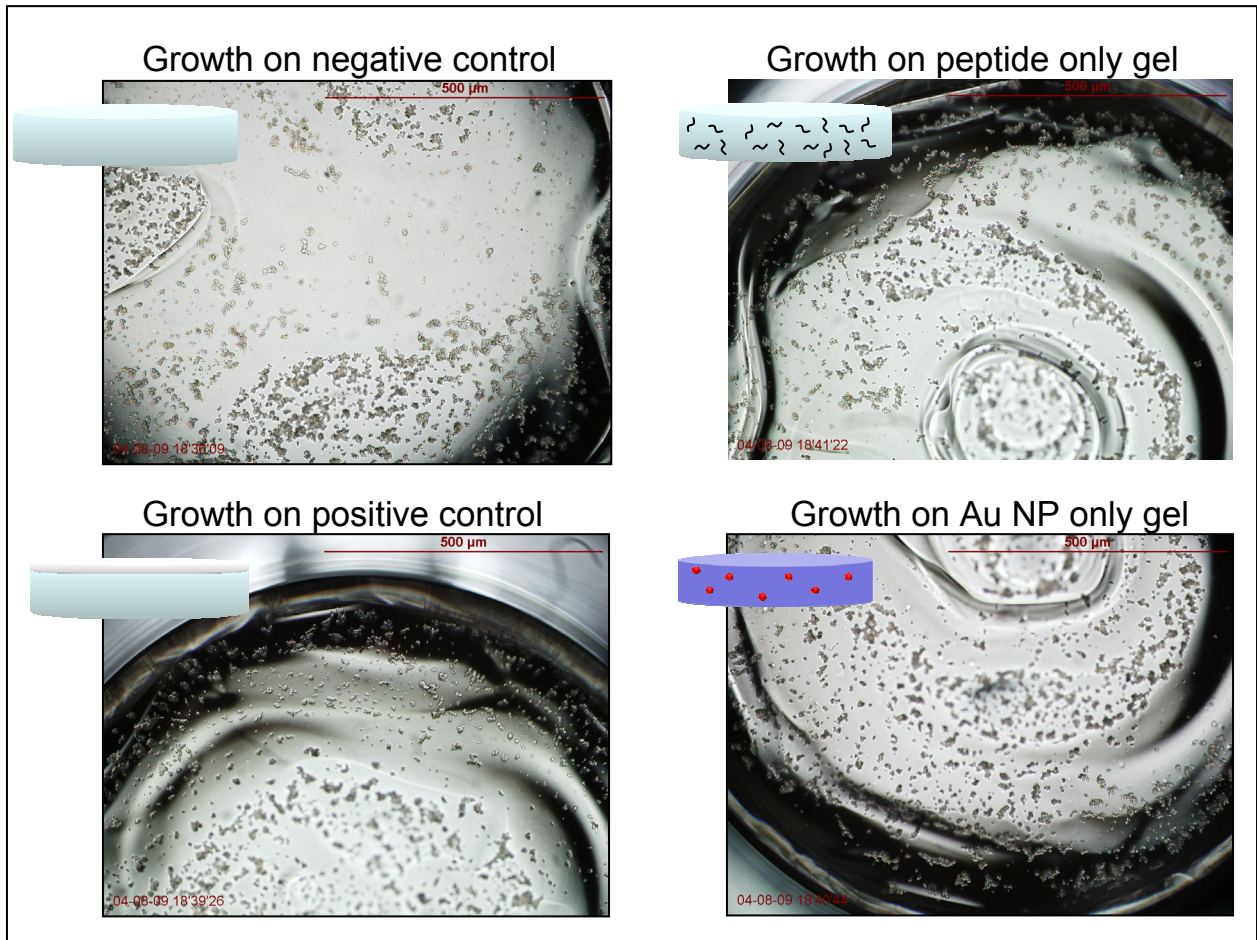


Figure 3.21: PEGDA Hydrogel (1x Au NP's) Cell Adhesion Images

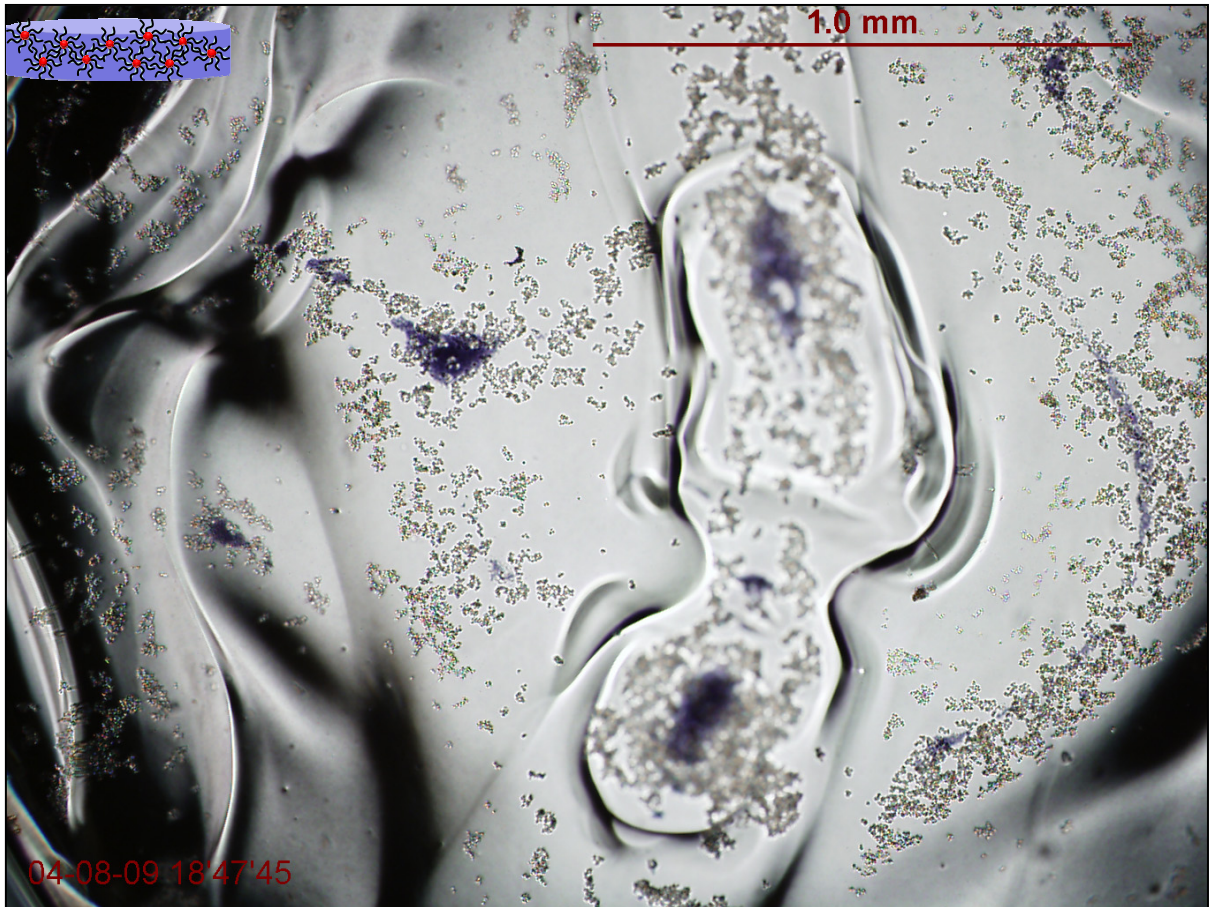


Figure 3.22: Experimental Composite PEGDA hydrogel (Au NP's and peptide)

3.4 Conclusions

An appropriate method (DMAA reduction) was selected to synthesize gold nanoparticles approximately 90-100 nm in diameter. Although the particles were not quite as monodisperse as a commercial comparison sample (90 nm Nanopartz), the resulting particles were still quite suitable for the applications where they would serve as anchors for cell adhesion peptides in a composite hydrogel. Approximately spherical gold nanoparticles with an average diameter of 90 nm were shown to remain entrained within the pores of agarose with minimal loss for a period of at least several days. While a small amount of initial particle loss occurred, the gels appeared to be stable for an extended period of time. Based on the pore structure of agarose and these results, any gold nanoparticles at least 90 nm in diameter or larger should also remain lodged inside the hydrogel. The composite hydrogels of various gold nanoparticle concentration were shown to not be statistically different in terms of their storage and loss moduli from the unmodified samples, although the standard deviation and sample to sample variation was very large. Because of this large variation, it cannot be concluded that the particles have no effect on the mechanical properties of the composite gels, but any effect is less than the sample-sample variation seen in forming the agarose hydrogels. The initial cell studies, while potentially demonstrating some positive results, are still inconclusive due to the need to fully quantify the extent of adhesion. This needs to be done in a consistent manner so that each sample receives the same shear stress during the key rinsing steps. While an improved testing procedure should yield more complete results, the comparison tests with PEGDA hydrogels show very promising behavior in the experimental sample with cells clustering around small aggregates of gold nanoparticles, perhaps indicating an adhesion preference. In the tests performed so far, both agarose and PEGDA

hydrogels have been modified with the proposed gold nanoparticle-based technique, indicating its flexibility to improve various types of biomaterials.

4. Biosensor

4.1 Introduction

Biosensors are quickly becoming prevalent in modern society and have many applications, including detecting biological hazards and diagnosing certain diseases. Nanoparticles, with their unique, size-dependent properties, are an extremely promising technology for biosensor creation. However, some of the most promising models employ aqueous unsupported nanoparticles which are difficult to adapt to applications outside of a laboratory. The proposed gold nanoparticle based technique of creating composite hydrogels and polymers can be applied to nanoparticle biosensing in order to develop a portable device with better commercial potential than unsupported liquid-based biosensors.

The proposed biosensor consists of gold nanoparticles modified in a similar method to that done in solution by Scrimin *et al* and West *et al*. However, this sensor will be embedded in a supporting polymer matrix which permits the development of portable devices with future potential for gas phase operation. The supporting matrix consists of poly(ethylene glycol) diacrylate (PEGDA) hydrogels chosen due to their robust nature in which particles can be easily embedded. Biosensor detection is based on the absorbance shift experienced by the gold nanoparticles, which is a function of their surface plasma resonance. By bringing two small gold nanoparticles (~15 nm) close enough together, the same shift in absorbance observed with large (80-100 nm particles) can be achieved as a result of the proximity of the small particles (Figure 4.1). If the particles are moved apart again, the absorbance shifts back to that of the small, separated particles. As a proof of principle case, the peptide (N term-CGGGRGDSGGGC-COOH term) is used to bind the nanoparticles together, and trypsin is used to cleave the peptide in the middle, returning particles to their initial unaggregated state. In this way, the sensor is

designed to detect the presence of trypsin. After the nanoparticles have been prepared with the linking peptide, they can be incorporated into the structure of a PEGDA hydrogel to provide the gel with sensing capability (Figure 4.2). Although this biosensor is still under develop, the initial tests to begin optimizing this system are described here.

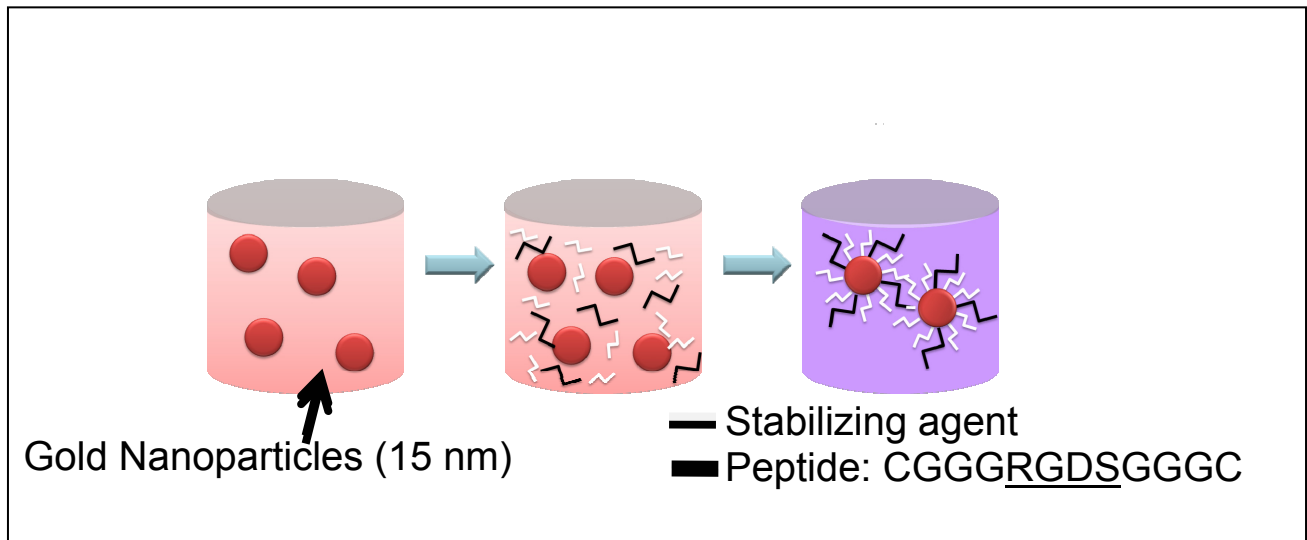


Figure 4.1: Peptide Binding Mechanism of Gold Nanoparticle Biosensor

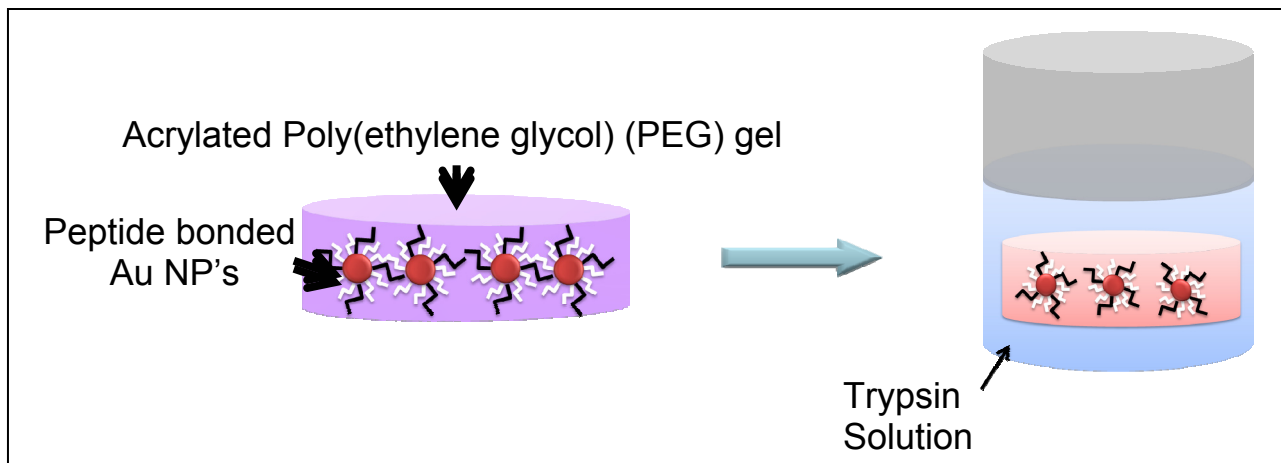


Figure 4.2: Converting Biosensor to Gel Basis and Sensing in Solution

4.2 Experimental

4.2.1 Initial Peptide Tests

Solutions of 15 nm gold nanoparticles [Ted Pella 15704] were tested with various concentrations of the peptide (N term-CGGGRGDSGGGC-COOH term) [95%, Genscript] to settle on an optimal ratio of adding 5 μL of 10 mg/mL peptide to 50 μL of the gold nanoparticles at their initial concentration. Absorbance spectrums were taken to analyze the solutions on a Genesys 6 UV-vis spectrophotometer [Thermo Electron Corp.]. Trypsin was tested at a ratio of 20 μL of 1.4 mg/mL solution added to 50 μL of the gold nanoparticles at their initial concentration. The gold nanoparticles were also tested by incorporating them into hydrogels formed by photopolymerizing poly(ethylene glycol) diacrylate (PEGDA) [MW 1000, Laysan Bio] in the manner described in Section 3.2.6.5. Results of these tests are detailed in Section 4.3.1

4.2.2 Stabilizing Ligand Tests

The following molecules were tested to determine which would be good candidates to serve as stabilizing ligands for the gold nanoparticles: 3-methyl-mercaptopropionic acid [Sigma Aldrich M5801], methyl-3-mercaptopropionate [Sigma Aldrich 108987], PEG (MW 8000, unmodified) [Sigma Aldrich P4463], Tween 20 [Sigma Aldrich P9416], and tri(ethylene glycol) mono-11-mercaptoundecyl ether (ME) [Sigma Aldrich 673110]. Various molar ratios (1:1, 10:1, 100:1, 1000:1, etc.) of supporting ligand to peptide (based on the level described in Section 4.2.1) were tested by creating the combined solutions and determining the absorbance as well as monitoring for aggregation or undesirable behavior.

4.2.3 Optimizing Stabilizing Ligand Concentration

After ME was selected as the optimal stabilizing ligand, further testing was performed to determine the minimum amount required to protect the gold nanoparticles from salt-induced aggregation. Combinations of solution were created with phosphate buffered saline (PBS) [Sigma Aldrich P3813] levels ranging from 0.001 M to 0.004 M and ME levels ranging from 8×10^{-8} to 8×10^{-6} M. Absorbance readings were taken for each sample to determine the optimal ME level.

4.3 Results and Discussion

4.3.1 Initial Peptide Tests

Figure 4.3 below shows the observed shift in absorbance of the 15 nm gold nanoparticles upon the addition of the CGGGRGDSGGGC peptide. A nanoparticle sample diluted to the same concentration as after peptide addition is included for reference. Although the absorbance peak widens with the addition of the peptide, its shift is very far from its original position and easily detectable. However, no change in the absorbance curve was found when Trypsin was added to attempt to return the nanoparticles to their original state. The wide absorbance curve for the peptide sample also indicates that the addition of the peptide is likely causing a range of particles to bind together. While this is less ideal, it is not problematic if the protease can still cleave the peptide linkages between nanoparticles. After modifying the gold nanoparticle solution with the CGGGRGDSGGGC peptide, aggregation continues beyond the initial color change and continues until within a few hours the solution appears clear and contains black deposits of severely aggregated particles at the bottom of the sample. This behavior along with the lack of effectiveness of the Trypsin, indicates that the particles aren't well stabilized and are aggregating to a large enough extent that even if the peptide bonds were cleaved, the particles would be unlikely to separate. Addition of salts, such as PBS, also shift the color of the 15 nm gold nanoparticle solution to a deep blue because of the interference of the ions with the electrostatic repulsions that keep the nanoparticles stabilized (Figure 4.4). This is also problematic as most biological applications will require at least weak salt buffers. An unwanted color change is also observed when the particles are integrated into PEGDA hydrogels where the red solution is converted to a blue-purple gel due to the PEGDA molecules interacting with the nanoparticles before the solution can be polymerized (Figure 4.5). All of this information points to the need for

an additional stabilizing ligand to be added to the gold nanoparticles so that they can resist the effects of ions in solution and remain able to separate into individual particles again if the linking peptide is cleaved.

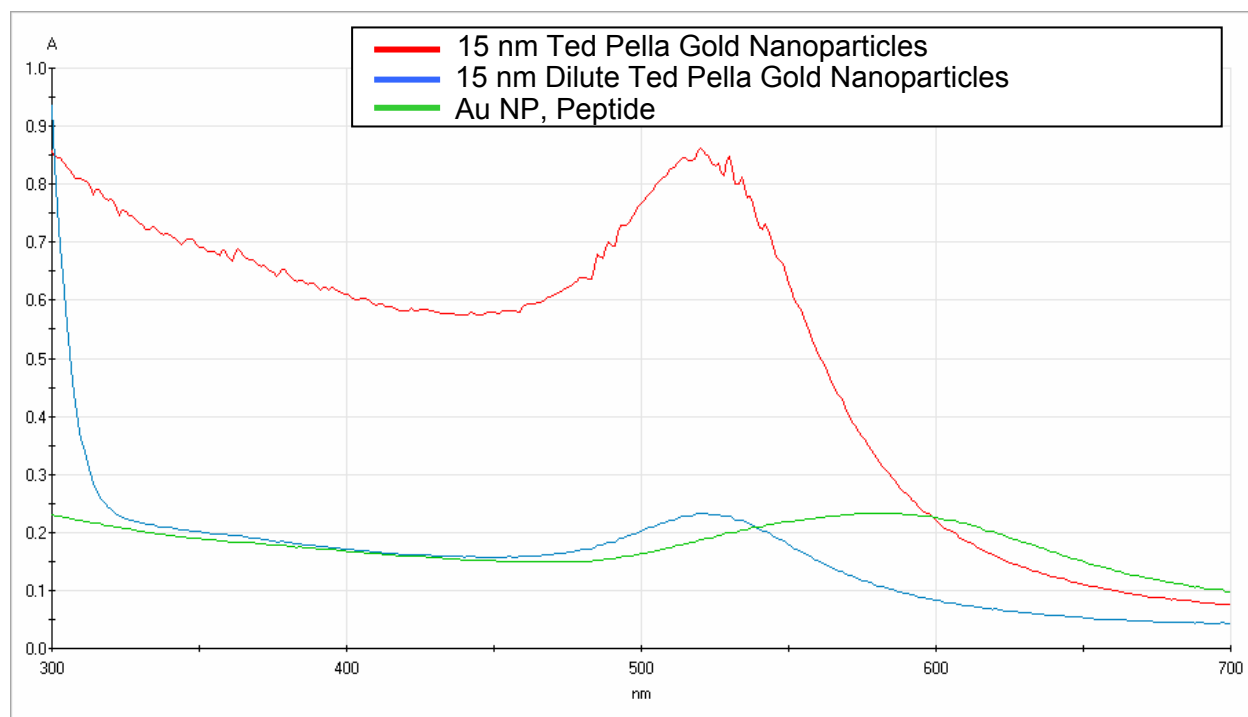


Figure 4.3: Absorbance Curves for Biosensor Peptide Addition

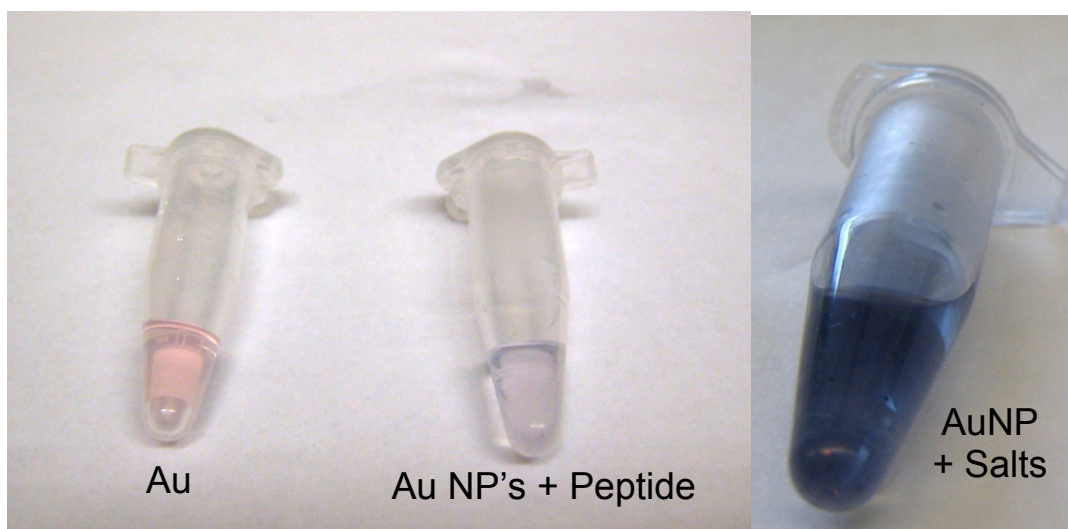


Figure 4.4: Comparison of Unmodified and Modified Gold Nanoparticles

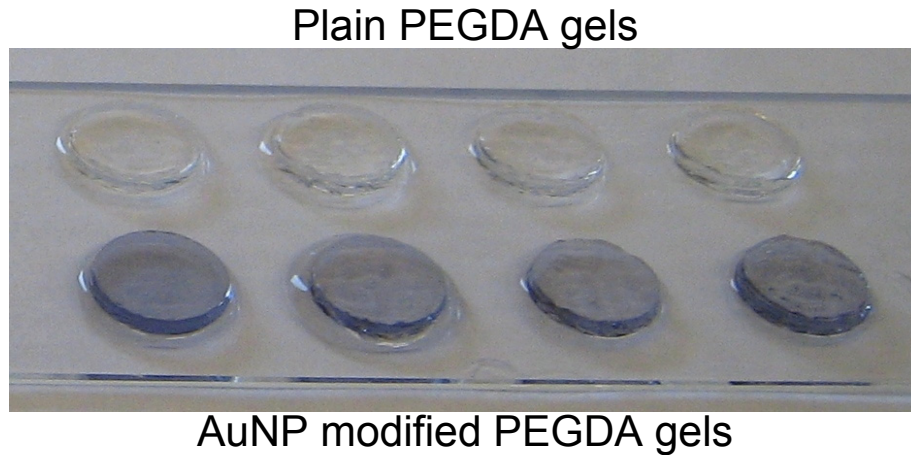


Figure 4.5: Unmodified and 15 nm Gold Nanoparticle Modified PEGDA Hydrogels

4.3.2 Stabilizing Ligand Tests

The ideal stabilizing ligand for the gold nanoparticles will have the properties described by Figure 4.6. One end will have a thiol group so that it may bind to the nanoparticle surface. The length of the ligand is also very important, as a ligand that is too short won't provide adequate steric interactions to keep the particles apart, and a ligand that is too long will interfere with the ability of the peptide to bind the nanoparticles together.

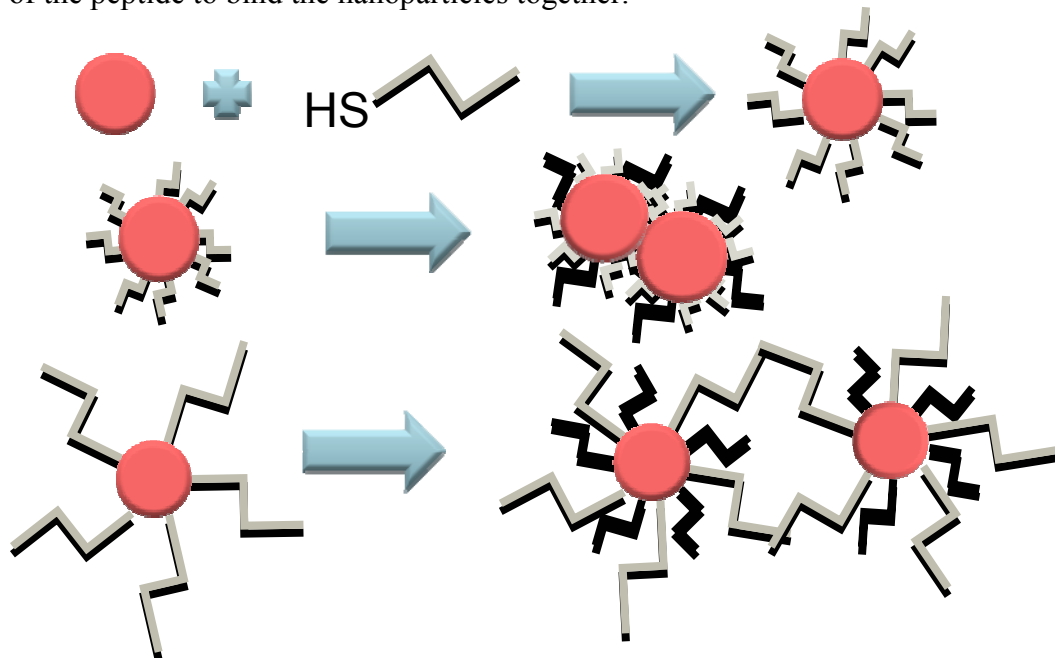


Figure 4.6: Schematic of Stabilizing Ligand Properties (ligand in gray, peptide in black)

Several potential ligands were tested, and their structures are shown in Figure 4.7. 3-methyl-mercaptopropionic acid by itself actually changed the color of the gold nanoparticle solution due to its weak acidic nature. Methyl-3-mercaptiopropionate, although able to bind to the nanoparticles and not containing the acid group of the previous ligand, did not provide any increase in stability for the nanoparticle solutions. Various chain lengths of unmodified PEG were equally ineffective. This was expected due to the non-thiolated nature of the PEG, but if the presence of the long chains in solution had helped to stabilize the nanoparticles, it would have provided an inexpensive protecting ligand. The surfactant Tween was also tested with slight signs of success, probably due to its ability to form micelles because of the mix of hydrophilic and hydrophobic groups. Based on these tests, the ideal stabilizing ligand was refined to a thiolated molecule with a hydrophobic inner group and a PEG-like hydrophilic outer group. The length of the molecule shouldn't be much more than a 20 carbon chain so as not to interfere with the peptide binding. The molecule tri(ethylene glycol) mono-11-mercaptoundecyl ether (ME) shown in Figure 4.8 fits these characteristics.

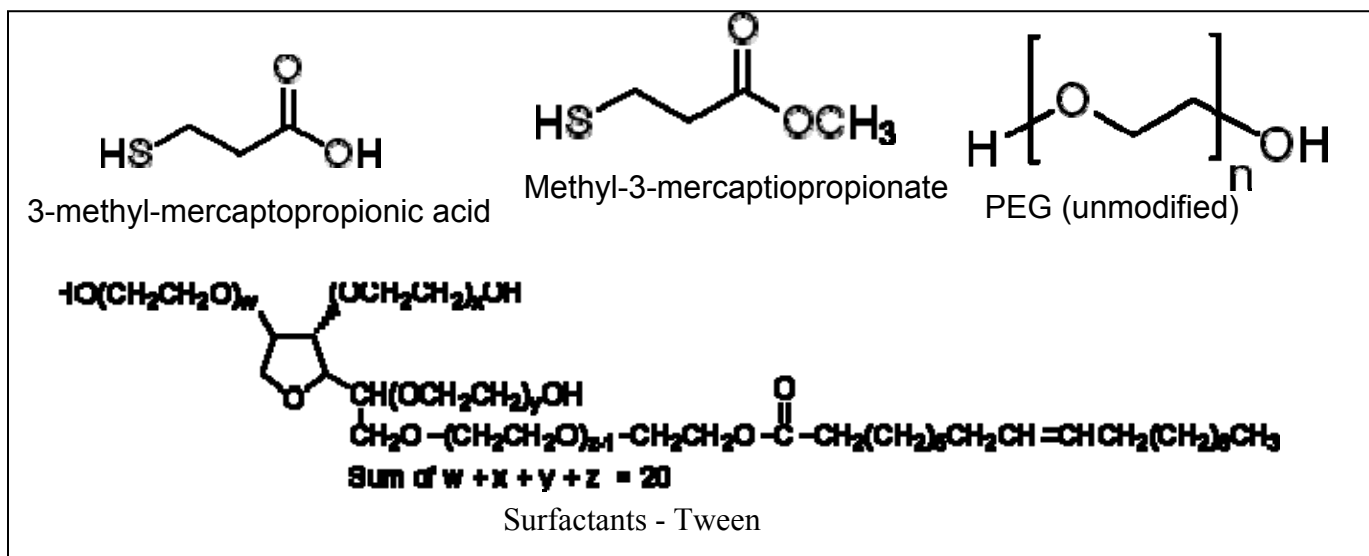


Figure 4.7: Structures of Unsuccessful Ligands



Figure 4.8: Tri(ethylene glycol) mono-11-mercaptoundecyl ether (ME)

4.2.3 Optimizing Stabilizing Ligand Concentration

The tri(ethylene glycol) mono-11-mercaptoundecyl ether (ME) molecule was further tested to determine the minimum concentration required to be an effective stabilizing ligand since a delicate balance is required between stabilizing the nanoparticles and covering too many of the available sites for sufficient peptide binding. The results of these tests are shown in Figure 4.9 where increasing concentrations of ME were tested against increasing concentrations of PBS in 15 nm gold nanoparticles. (All concentrations listed are the final solution concentration.) Absorbance spectrums for these tests are also included in Figures 4.10 through 4.12. Only dilute concentrations of PBS were tested to correspond with working with potential biological solutions in dilute buffers. Without any ligand, the nanoparticles are adversely affected by the PBS by the time it reaches 0.002 M with a complete shift to blue by 0.004 M. The addition of 8×10^{-8} M ME begins to have a slight protecting effect on the nanoparticles, as evidenced by the slight increase in peak absorbance between Figure 4.11 and 4.10. Since the ions from PBS interfere with the electrostatic repulsions stabilizing the 15 nm gold nanoparticles, the particles will begin to aggregate in collections of various sizes, destroying the distinctive absorbance peak of monodisperse gold nanoparticles. As seen in Figure 4.12, by the time the ME concentration has reached 8×10^{-6} M, the absorbance curves of the PBS modified solutions are only minimally affected. This indicates that a concentration of 8×10^{-6} M ME can protect 15 nm gold nanoparticles against at least a 0.004 M solution of PBS equivalent ion concentration.

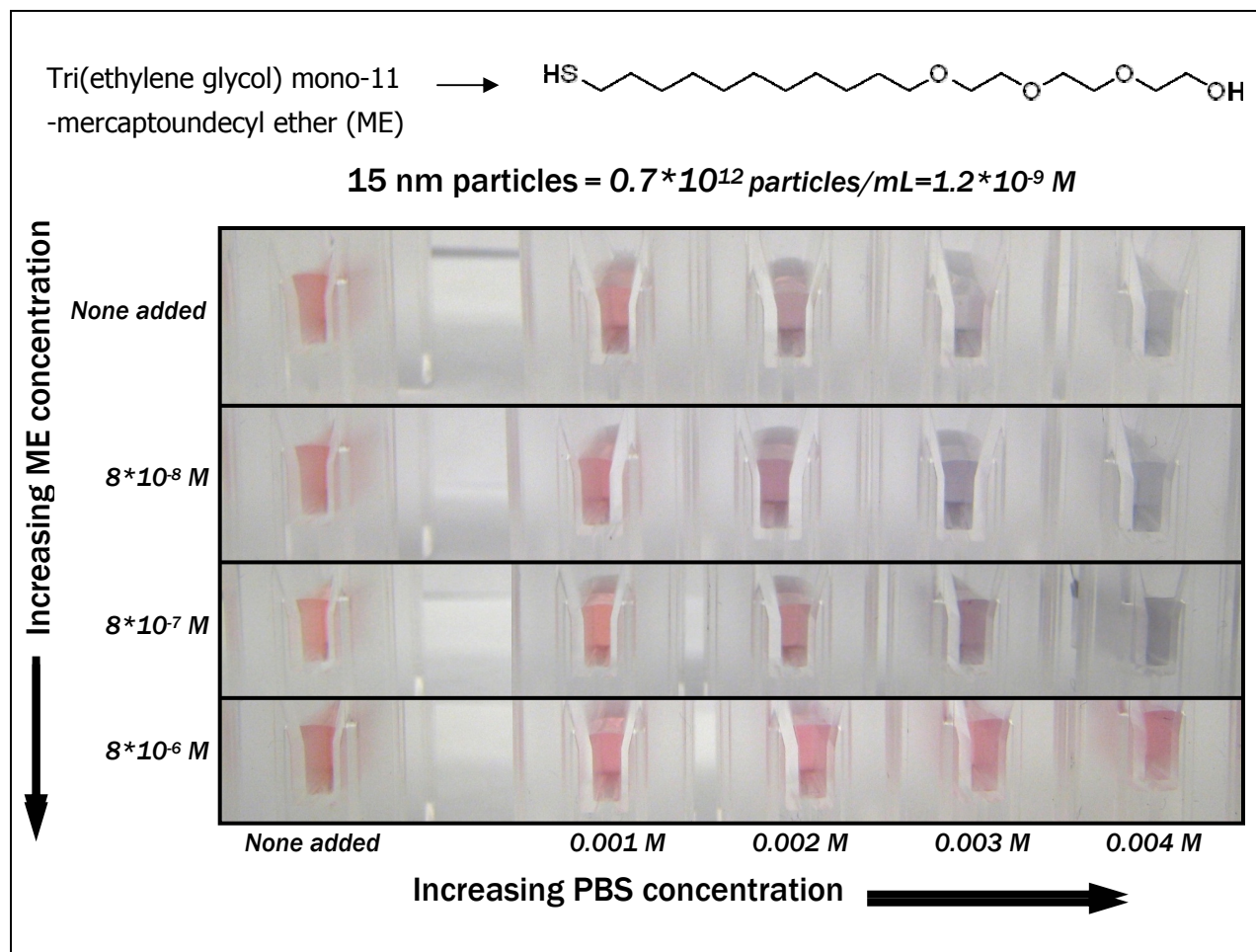


Figure 4.9: Combined Effect of ME and PBS on 15 nm Gold Nanoparticles

Figure 4.13 compares the absorbance spectrums of unmodified 15 nm gold nanoparticles with ME protected and unprotected gold nanoparticles once the CGGGRGDSGGGC linking peptide was added. The unprotected peptide modified particles exhibit the expected absorbance peak, but the ME protected particles only show a slight shift from the unmodified particles with lower concentrations of ME leading to a slightly larger shift. While this situation is less than ideal and makes visual distinction more difficult when ME is used, the difference can easily be resolved if an absorbance spectrum is taken. Although the presence of ME stabilizes the particles against unwanted color changes, it also stabilizes to a degree against the desired shift from the presence of the peptide. Additional testing with different length ligands similar to ME or different length

peptides is necessary to further improve the performance of the sensor in the liquid phase before further experimentation is done with a gel-based sensor.

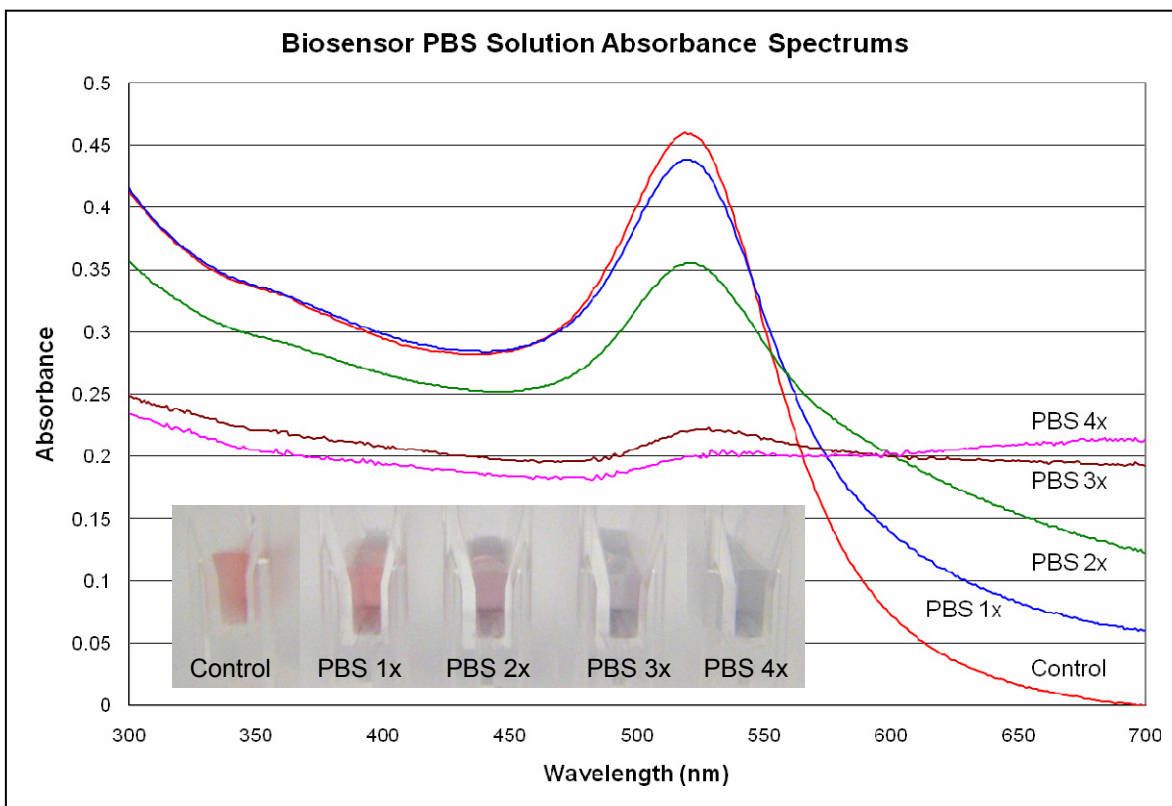


Figure 4.10: Absorbance Spectrums with No ME and Increasing PBS

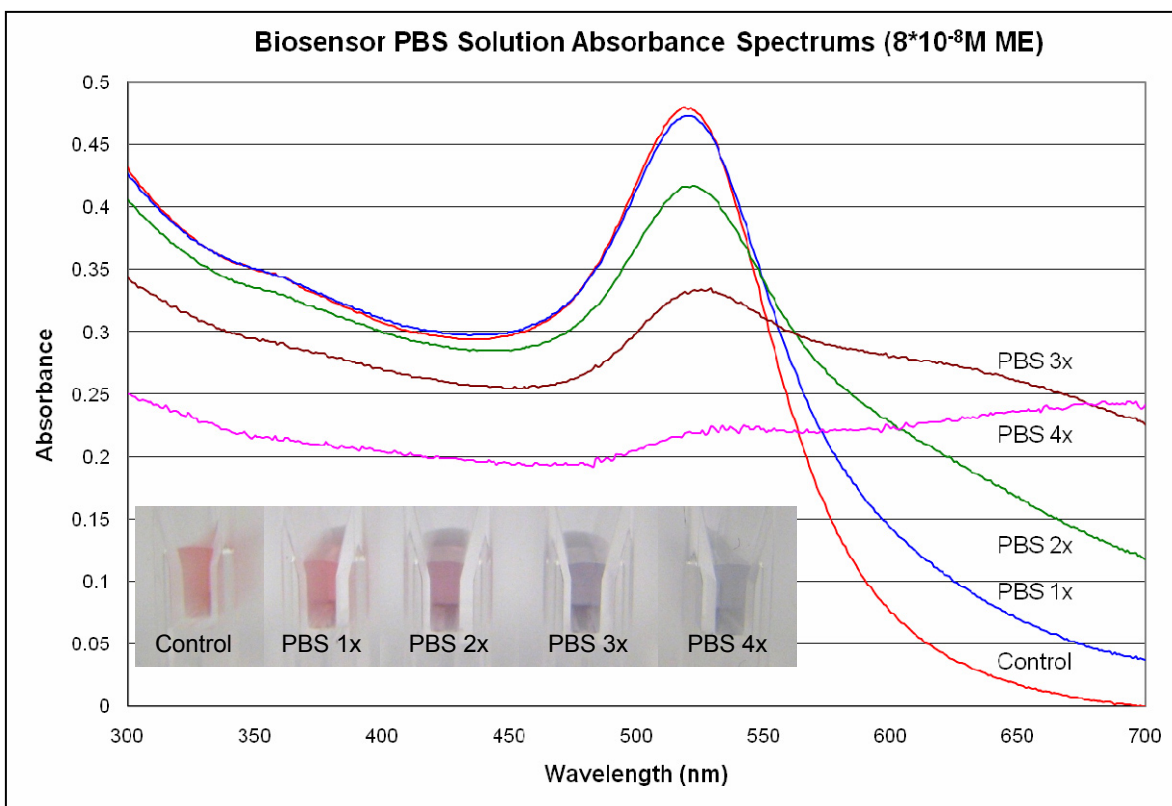


Figure 4.11: Absorbance Spectrums with 8×10^{-8} M ME and Increasing PBS

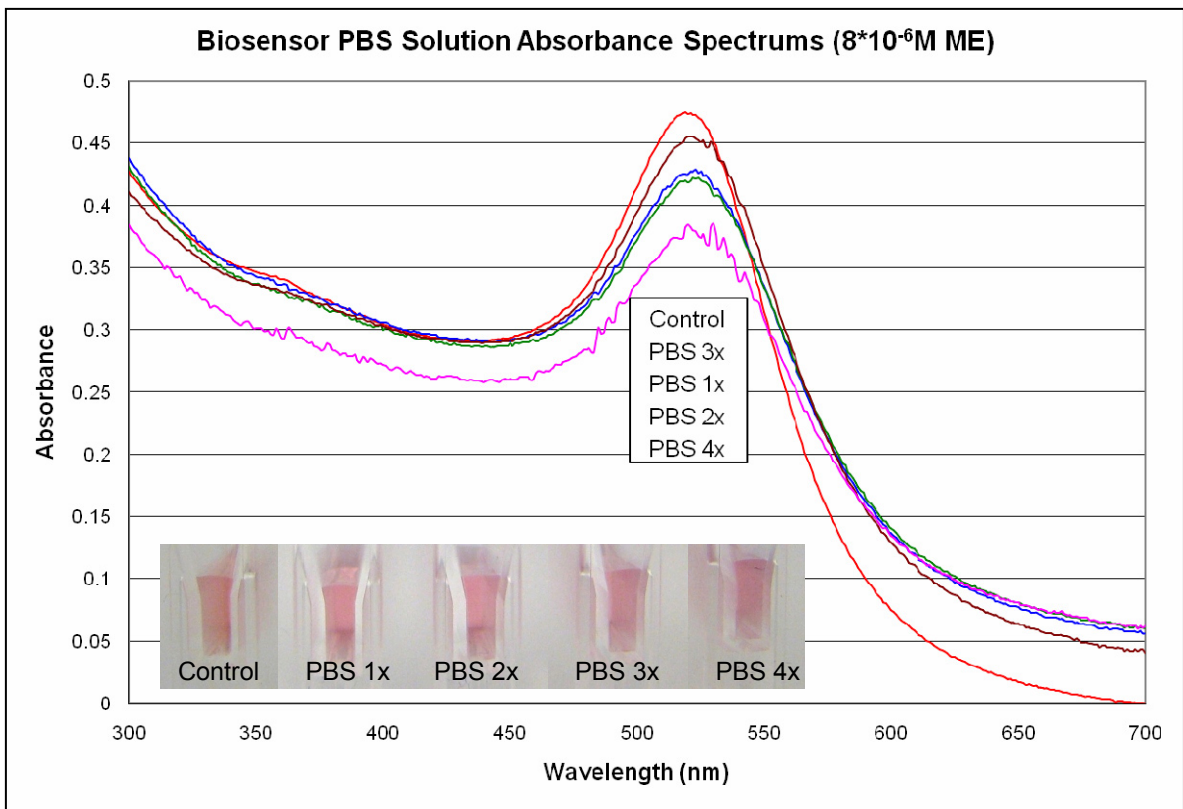


Figure 4.12: Absorbance Spectrums with $8 \times 10^{-6} \text{ M ME}$ and Increasing PBS

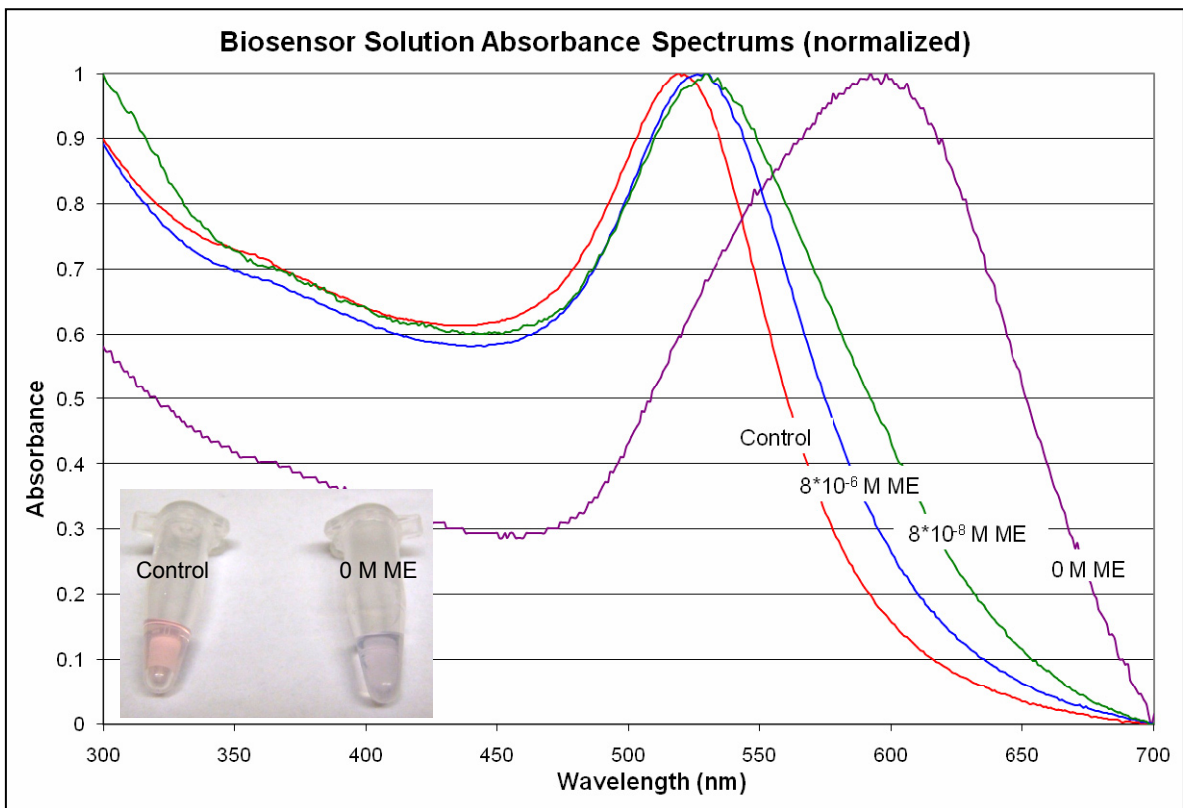


Figure 4.13: Normalized Absorbance Spectrums with ME and Peptide added

4.4 Conclusions

Gold nanoparticles have successfully been conjugated using the CGGGRGDSGGGC peptide and shown to exhibit a distinct color and absorbance difference before and after conjugation. However, the particles are not stable enough for biological applications or to complete the second part of the sensing reaction without the presence of an additional stabilizing ligand. After testing several potential candidates, an ideal ligand was found to be tri(ethylene glycol) mono-11-mercaptoundecyl ether (ME). This ligand has a thiol group to bind directly to the gold nanoparticles, followed by a hydrophobic and then a hydrophilic section to better disperse the ligand on the particle surface while still allowing it to interact favorably with the water molecules surrounding the particles. ME is also a suitable length based on the peptide being tested. A concentration of 8×10^{-6} M ME was found to provide strong protection for the particles from PBS-like ionic solutions at concentrations of at least 0.004 M. Unfortunately, the presence of ME reduces the absorbance shift caused by the addition of the linking peptide. This change makes visual recognition of the sensor more difficult, but the difference can easily be resolved using the appropriate instruments. At this point, further testing is required to fully optimize the biosensor in liquid form before transferring to a hydrogel basis, but the work in stabilizing the sensor is also necessary in the gel platform and will directly transfer over. The ME ligand was also found to be ideal for this application, and it is commercially available compared to the more common lengthy synthesis processes used to create short thiol-based stabilizing ligands.

5. Overall Conclusions

Although the gold nanoparticle based approach of creating composite biomaterials with additional functionality is still undergoing development, the results to date are promising. Gold nanoparticles of the appropriate size have been synthesized by modifying an adaptive temperature controlled technique. Composite gold nanoparticle – agarose hydrogels have been created and tested to show that the bulk of particles remain in the gel for a substantial length of time, and the mechanical properties of the composite hydrogels are similar to the unmodified hydrogels, retaining the native material characteristics. A cell-binding peptide has successfully been conjugated to the gold nanoparticles, and the effect of this binding peptide on cell growth and adhesion has been studied by culturing cells on the unmodified and composite hydrogels. While the initial results are promising, more testing is necessary to quantify the extent of adhesion in each case. However, the incidence of larger cell clumps and the tendency of cells to cluster around small aggregates of the modified gold nanoparticles indicate that composite system is having an effect on the cell behavior.

Gold nanoparticles have also successfully been conjugated using the CGGGRGDSGGGC peptide to provide the first component of the sensing reaction. The commercially available ligand tri(ethylene glycol) mono-11-mercaptoundecyl ether (ME) has been tested and found to be an excellent stabilizing ligand for the particles. With the presence of this ligand, future testing can focus on optimizing the peptide cleaving reaction in solution and then transferring to the hydrogel platform. Since small (~15 nm) gold nanoparticles were observed to aggregate to a degree in forming PEGDA gels, the data from the ME optimization experiments can also apply to the cell adhesion application of the gold nanoparticle biomaterial composites in order to reduce unwanted aggregation in forming certain types of hydrogels.

Although additional work is required to complete the two proposed composite systems, the progress to date indicates the feasibility of these systems. The hydrogel biomaterials gain increased functionality without the requirement of complicated syntheses, and the nanoparticles are provided with a supportive framework. The methods described here are also very flexible as a result of the ability to functionalize the gold nanoparticles with a wide array of biomolecules, providing a composite system with a variety of features in a way that applies equally well to a range of materials. The potential applications of this approach, from tissue engineering to three dimensional cell studies to biosensing, are strong motivations for further investigation of this model system.

6. Recommendations for Future Work

In order to complete the gold nanoparticle-hydrogel composite system, work remains in a few key areas. The cell adhesion application requires additional quantitative adhesion studies to confirm the effectiveness of the new technique. While conducting this test in a consistent manner has been hampered by the intricacies of working with the hydrogels and the requirements of the biological system, performing future tests in a customized microfluidic device would be an ideal way to achieve the desired control and consistency. The extent of peptide attachment to the gold nanoparticles also needs to be quantified to better compare the proposed method to existing literature. This may be achieved through more conventional approaches, such as the Bradford assay, as well as through radiolabeling. This will also allow for determining the effect of ligand density and spacing on cell adhesion when this information is correlated with nanoparticle concentration. Once the cell adhesion platform is better characterized, additional studies can be performed with encapsulated cells and PC12 cells exposed to nerve growth factor to determine the effect of the system on neurite extension. For the biosensing aspect of the composite platform, the optimization of the stabilizing ligand will allow for the completion of the solution-based tests before integrating it into the hydrogel system.

7. References

- ¹ Gasser, T. (2005). Genetics of Parkinson's disease. *Curr Opin Neurol*, 18(4), 363-369.
- ² Breit, S., Schulz, J.B., Benabid, A.L. (2004). Deep brain stimulation. *Cell Tissue Res*, 318(1), 275-288.
- ³ Moss *et al.* (2004) *Brain*. 2755.
- ⁴ Cukierman, E. Pankov, R., Stevens, D., Yamada, K. (2001). Taking cell-matrix adhesions to the third dimension. *American Association for the Advancement of Science. Science*, 294(5547), 1708-1712.
- ⁵ Discher, D., Janmey, P., Wang, Y.L. (2005). Tissue cells feel and respond to the stiffness of their substrate. *Science*, 310(5751), 1139-1143.
- ⁶ Fatin-Rouge, N., Starchev, K., Buffle, J. (2004). Size effects on diffusion processes within agarose gels. *Biophysical Journal*, 86, 2710-2719.
- ⁷ Phillips, G., Williams, P. (2000) *Handbook of Hydrocolloids*.
- ⁸ Bellamkonda, R., Ranieri, J.P., Aebischer, P. (1995). Laminin oligopeptide derivatized agarose gels allow 3-dimensional neurite extension in-vitro. *Journal of Neuroscience Research*, 41(4), 501-509.
- ⁹ Mann, B., Gobin, A., Tsai, A., Schmedlen, R., West, J. (2001). Smooth muscle cell growth in photopolymerized hydrogels with cell adhesive and proteolytically degradable domains: synthetic ECM analogs for tissue engineering. *Biomaterials*, 22(22), 3045-3051.
- ¹⁰ Hsiong, S.X., Cooke, P.H., Kong, H., Fishman, M.L., Ericsson, M., Mooney, D.J. (2008) AFM imaging of RGD presenting synthetic extracellular matrix using gold nanoparticles. *Macromolecular Bioscience*, 8, 469-477.
- ¹¹ Chithrani, B.D., Chan, W. C. (2007) Elucidating the mechanism of cellular uptake and removal of protein-coated gold nanoparticles of different sizes and shapes. *Nano Letters*, 7(6), 1542-1550.
- ¹² Song, J., Kim, Y., Kim, J. (2006) Synthesis of gold nanoparticles using N,N-dimethylacetoacetamide: Size and shape control by the reaction temperature. *Current Applied Physics*, 6(2), 216-218.
- ¹³ *Nanopartz Accurate Spherical Gold Nanoparticles*. Nanopartz: The Gold Nanoparticle for Nanotechnology. Product Specifications, 2009. (http://www.nanopartz.com/Bare_Spherical_Gold_Nanoparticles.htm)
- ¹⁴ Guarise, C., Pasquato, L., Scrimin, P.S. (2005) Reversible aggregation/deaggregation of gold nanoparticles induced by a cleavable dithiol linker. *Langmuir*, 21, 5537-5541.
- ¹⁵ Guarise, C., Pasquato, L., De Filippis, V., Scrimin, P. (2006) Gold nanoparticles-based protease assay. *PNAS*, 103(11), 3978-3982.
- ¹⁶ Chang, E., Miller, J.S., Sun, J., Yu, W.W., Colvin, V.L., Drezek, R., West, J.L. Protease-activated quantum dot probes. *Biochemical and Biophysical Research Communications*, 334, 1317-1321.
- ¹⁷ Seaprep® Agarose: An ultralow gelling, soft agarose. Lonza Rockland, Inc., product insert, 2007. Document # 18842-1007-02.
- ¹⁸ Markgraf, W., Horn, R. An introduction to rheology in soil mechanics – Structural behavior of bentonite against salt concentrations and water content. Christian-Albrechts-University of Kiel: Institute for Plant Nutrition and Soil Science.

